

# **Aerodynamically Adaptive Bodies**

Submitted in partial fulfillment of the requirements

of the degree of

(Bachelor of Engineering)

by

**1. Shubham Sharad Kothawade** 72034068D

**2. Omkar Ashok Bhise** 71841710M

**3. Rohit Khandu Galande** 71841577K

Under the valuable guidance of

**Dr. Manoj Nagmode**



(Department of Electronics & Telecommunications)

**Government College of Engineering and Research, Avasari (Kh),  
Taluqa: Ambegaon, District: Pune**

**(SAVITRIBAI PHULE PUNE UNIVERSITY, PUNE)**

**(June, 2023)**

# INDEX

## Contents

ACKNOWLEDGEMENT .....	5
INDEX .....	6
Abstract.....	7
Chapter 1: Introduction .....	8
Chapter 2: Literature Review.....	10
Chapter 3: Proposed Solution .....	17
Chapter 4: Mechanism and Working .....	27
Chapter 5:.....	35
Components Used.....	35
Schematic / Circuit.....	47
Scope of Development:.....	49
References:.....	51

## Abstract

Nowadays, modern trucks are equipped with a number of drag-reducing mechanisms. Many numerical and experimental studies of the aerodynamics of heavy vehicles have been carried out. Most of today's research is focused on reducing drag in newly designed trucks. As a result, little work is done on current designs. Due to the high number of trucks already on the road today, as well as the fact that many of these older designs are still being sold, it is necessary to find ways to reduce the drag of these designs.

Fleet managers know that drag (wind resistance) is responsible for most of the energy loss from trucks on highways. Reduced drag improves fuel economy. The longer the distance traveled and the higher the speed, the greater the potential for increased efficiency. Over the last 20 years, manufacturers have made great strides in reducing the drag coefficient (a measure of drag) of a typical truck from about 0.8 to about 0.65. This is an improvement of nearly 20%. The Environmental Protection Agency (EPA) says further efforts to improve aerodynamics could reduce drag by another 25%. This can have a significant impact on fuel consumption. For example, according to the agency, a 20% reduction in air resistance can improve fuel efficiency on the highway by up to 15%. There are many options to improve aerodynamics and improve fuel economy. Truck/trailer aerodynamics includes many changes to roof panels, side panels, side tank panels, aerodynamic front bumpers and mirrors. Trailer aerodynamic options include side skirts or chassis, wheel covers and trailer tails. Aerodynamic long range station wagon can achieve 11% fuel savings compared to typical long range station wagon. The result is approximately 1,600 gallons. Saved over \$6,000 in fuel costs and 16 tons of carbon dioxide.

This project focuses to study the existing solutions through a deep literature study and finally build a prototype which will eliminate almost all the problems which were found in the past systems. A rigorous testing and analysis of model is under process and is awaiting for the expected results.

## Chapter 1: Introduction

Full automotive field is continuously under development since decades. Every day comes up with new and unique problem statement followed by series of solutions from the engineers all around the globe. Considering the mentioned problem statement viz. Staggered aerodynamics of a moving body, several solutions have been implemented till date in order to reduce the aerodynamic drag on the moving body. Few of them which were referred for the project are described sequentially.

Aerodynamic drag is the force that prevents an object from moving. When a vehicle, regardless of size, is designed to allow air to flow over its body, aerodynamic drag will have less of an impact on its performance and fuel economy. Heavy trucks burn a significant amount of fuel to overcome air resistance. More than 50% of an 18-wheeler's fuel is used to reduce drag on highways.

Recent research into truck fuel economy technologies shows that aerodynamic optimization is one of the most important technologies when it comes to fuel economy. A large commercial vehicle traveling at 100 km/h uses about 50% of its total fuel to provide the power needed to overcome aerodynamic drag. The average annual mileage of a heavy commercial vehicle was found to be between 130,000 km and 160,000 km. With such a high mileage, any reduction in drag will result in significant fuel savings and reduced greenhouse gas emissions. This is also related to the high level of pollution (CO<sub>2</sub>) from the burning of fossil fuels. Their results show that improvements in fuel consumption can be achieved from less than 1% to almost 9% of annual mileage. The field of aerodynamics plays an important role in the design and operation of many vehicles, models and systems. Traditionally, the aerodynamic shape and configuration have been optimized for specific operating conditions, resulting in reduced overall performance. However, recent advances in data, sensors and technology have led to the development of modified aerodynamic bodies that can change their shape and behavioural set in response to changes. These modified systems have the potential to transform performance, mobility and safety in a wide range of applications, from aircraft and cars to wind turbines and toys.

To overcome the problem of loss of economy, efficiency and performance we have proposed a system of **Aerodynamically Adaptive Bodies**.

## **Objectives**

The primary objective of this project report is to explore the concept and potential applications of adaptive aerodynamic bodies. Specifically, the report aims to:

- Provide an overview of the fundamental principles and theories behind adaptive aerodynamics.
- Examine the various types of adaptive systems and their working mechanisms.
- Highlight the advantages and challenges associated with adaptive aerodynamic bodies.
- Discuss the current state-of-the-art technologies and research efforts in this field.
- Present case studies and examples of successful applications of adaptive aerodynamics.
- Evaluate the potential future developments and implications of adaptive aerodynamic bodies.

## Chapter 2: Literature Review

Increasing the fuel efficiency and reducing the drag has been trailed since decades. Various systems were proposed and also used on the different types of vehicles. Few of the systems which were referred for the project are described sequentially.

Chief Engineer **Mauro Forghieri** in late 1960's came up with a system similar to one which now we all call as the Drag Reduction System (DRS). It was the combination of three switches in which two were automatic and one was the manual one. the first automatic was connected to the gear lever and only worked when using the first three gears to increase acceleration out of corners. The second automatic was connected to the brake pedal and worked the same as the solution from **Matra (Matra International team)**, it worked when braking. Then the manual one, which was activated only when the driver needed it; this was designed for high-speed cornering where the driver would not be using the brake pedal or downshifting, allowing them more grip when needed.

Recently, few of the systems are proposed with the purpose of reducing aerodynamic drag of the heavy vehicle viz,

**Adding a Deflector:** The most popular accessory is the deflector, which is a flat and shaped plate attached to the top of the cab at various angles. It is added to a simple box model and then meshed. Finally, current flow is passed through to evaluate the drag reduction effect of this kit.

**Traps / Basic flaps** are simple trapezoidal plates installed on the bottom of the container and converge to delay separation and control turbulence. It is known from the literature that the effect of basic flaps depends on the Reynolds number and the relationships are thus complicated.

**Cab vanes** are curves in the front of the body that reduce the frontal area, thereby reducing air resistance and deflecting the streamlines away from the truck.

**Front splitter** It is used for a smooth flow of air under the vehicle so that it cannot be deflected or obstructed by various devices under the vehicle. ~ **Reduction of Aerodynamic Drag of Heavy Vehicles (IJRASET 2021)**

**Spoiler:** It is one of the most used and important aerodynamic devices in the automotive domain. Its main purpose is to "spoil" unwanted air flow and direct good air flow, helping to reduce drag. However, the real use of the spoiler is evident at higher speeds above approximately 120 km/h. Commercial vehicles typically use it to increase the appeal of the vehicle's design, providing little or no aerodynamic advantage. Mainly high-performance vehicles therefore adapt it to reach higher speeds. The low-pressure zone behind the vehicle is reduced, resulting in less turbulence, which in turn leads to a reduction in air resistance

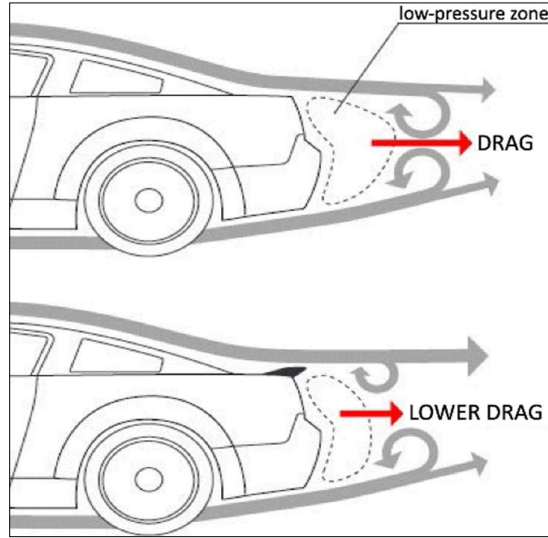


Fig 2.1

**Wing at the rear of a car:** A wing is another essential aerodynamic device that racing cars often use. The rear wing may look like a spoiler, but it differs in its function. It is shaped like an upside-down airplane wing. Its main purpose is to provide enough downforce or negative lift so that the vehicle has increased traction and the vehicle does not lift at higher speeds. It also enables faster cornering and improves stability at high speeds. But using a wing can add drag to the vehicle body. So, with any lift gained, drag also increases. This is generally considered a compromise between drag and lift.



Fig 2.2

**Fins:** Swedish hyper car manufacturer **Koenigsegg Automotive AB** testifies to the application of fins on the back of the car body.

Their flagship model "Jesko Absolut", which has the lowest drag coefficient in their lineup, has fins instead of a wing. The fins are inspired by fighter jets to provide stability at high speeds and reduce drag.



Fig 2.3

♣ **Front fairings and nose cones:** these are modifications to the front of the trailer, above the tractor cab, that direct airflow more smoothly over the trailer. They are generally curved, convex structures.

♣ **Side skirts:** like air dams on the tractor, these attach to the bottoms of the sides of the trailer and block airflow underneath the trailer, particularly in crosswinds.

♣ **Aerodynamic underbody:** the underbody of the trailer can be made more aerodynamic by adding fairings that redirect air around underbody components, such as wheels and axles.

♣ **Boat tails:** these are tapering extensions to the trailer that reduce the amount of wake at the rear of the vehicle. They are often inflatable, flexible, or retractable to make unloading easier.

♣ **Vortex generators:** the vortex generators mentioned in the truck section can also be installed on the back of the trailer, performing the same function by keeping high pressure air from entering the low-pressure wake and causing drag.

♣ **Pneumatic blowing:** this technology is not yet commercially available, but has performed well in tests. Air is blown from slits at the rear of the trailer, which causes the flow around the vehicle to be drawn in, diminishing the size of the wake.

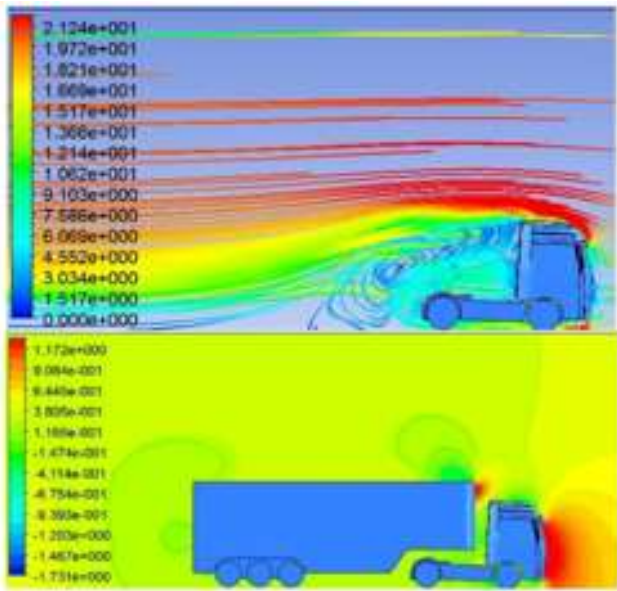


Fig 2.4

Rear spoilers are an extended part of the rear of the vehicle. A lot of "downforce" is needed at low speeds because the car is quite stable while moving. When speed increases, the rear spoilers increase the pressure on the rear wheels, fixing them to the ground and increasing stability and grip. The extent to which these rear spoilers are named varies from car manufacturer to car manufacturer. Leaning increases drag, which helps when using the brakes.

As we can see in the CFD analysis that the drag after the Trailor is attached to tractor is increased exponentially. If the tractor had an attachment which adjusted as per the current situation considering the wind direction, wind speed. This will bypass the coming wind force and hence will reduce the drag. Consequently, the fuel consumption will be on the lower end.



In the figure 2.5 we can see that the flow of turbulent air. In trucks, vehicle aerodynamics has a large effect on combustion, it is estimated that trucks use up to 40% of fuel just to overcome air resistance, if the kits were perfectly aerodynamic they

Fig 2.5

would use almost half as much fuel as now, showing that the potential savings lie in the shape of the car we drive, while perfectly aerodynamic vehicles are currently in the design phase, we can modify the kit in a short time to be more aerodynamic and use less fuel to install the

aerodynamic kit side fairing cab roof D turbulator z' and side skirts will help you save up to 10% fuel when installing these elements the size and shape of the trailer must be taken into account in addition the latest American invention wheel covers reduce combustion by about 3% it is worth it knowing that some other elements can increase combustion, you can save several hundred euros by removing the sun visor long distance driving laziness with the windows open increases combustion, which is equivalent to throwing a new mobile phone out the window every month, most exterior decorations such as protective frames or additional lights also increase combustion by a few percent, if you follow the above tips to significantly improve the aerodynamics of the vehicles in your company , you will save quite a large amount of money and ultimately help the environment.

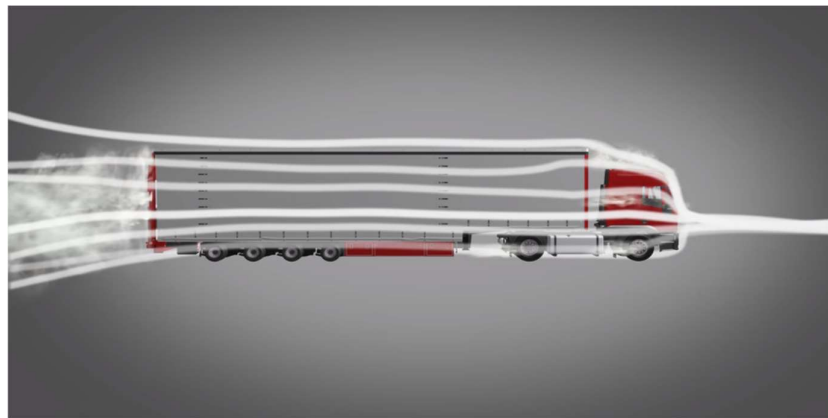


Fig 2.6



Fig 2.7

Wing flexibility plays a major role in aerodynamic systems, both natural and artificial, by increasing efficiency and mitigating damage to the structure under sudden loading. Effect wing flexibility has long been studied in the context of biolocomotion where it is known that flexibility has favorable aerodynamic and hydrodynamic properties.

There is an increasing need to develop unsteady aeroelastic models to realize these advantages engineering systems, such as for driving autonomous flying vehicles, including sizes comparable to insects and birds. The benefits of wing flexibility are often subtle consequences aeroelastic effects and for many applications it is also important to trap an unstable viscous fluid transient phenomena. This work develops accurate and efficient models to capture these effects in design and control effort.

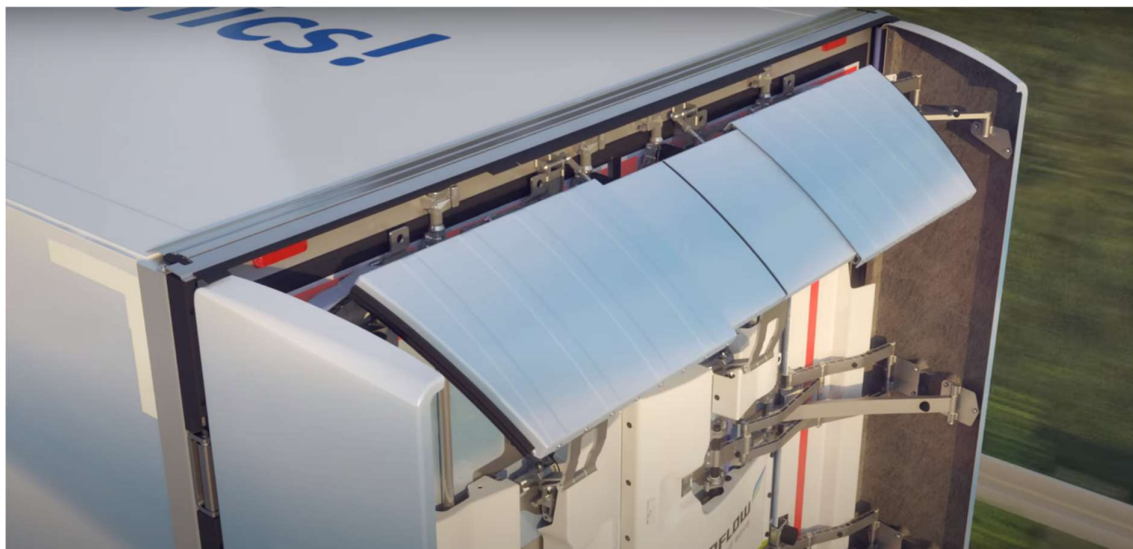


Fig 2.8



Fig 2.9

Heavy vehicles are aerodynamically inefficient due to their large frontal area and blunt body shape compared to other ground vehicles. A 40-ton semi-truck traveling at 60 miles per hour is estimated to use about 34 liters of fuel to overcome the drag of a 100-mile highway strip. The average car consumes a quarter less under similar conditions. Additionally, national fuel spending on road vehicles can be heavily skewed toward heavier vehicles. The drag-reducing mods have matured well over the decades and have significantly improved aerodynamics. Drag in heavy-duty vehicles is typically reduced through a variety of approaches, including streamlining airflow, reducing eddy current and flow separation, and masking exposed underbody structures. These can be accessed through cab and trailer mounted devices such as cab roof and side panels, tractor and trailer side skirts, trailer front panels, vortex generators and floor hatches.

## Chapter 3: Proposed Solution

As the title '*Aerodynamically adaptive bodies*' gives an idea that the proposed solution is something which is relative in nature and adaptive with changing aerodynamic conditions. As we observed that the traditional methods for reducing aerodynamic drag were designed for the ideal condition which was occurring at maximum frequencies in the time period of product life. This was not useful when the conditions were different from the ideal conditions. Unlike that, we are now with the solution which will be adaptive in nature. The system will also work with varying conditions and Realtime changes will be implemented on the moving system. For the project we have considered an example of the heavy truck carrying load. This will give us an visual of the problem and proposed solutions.

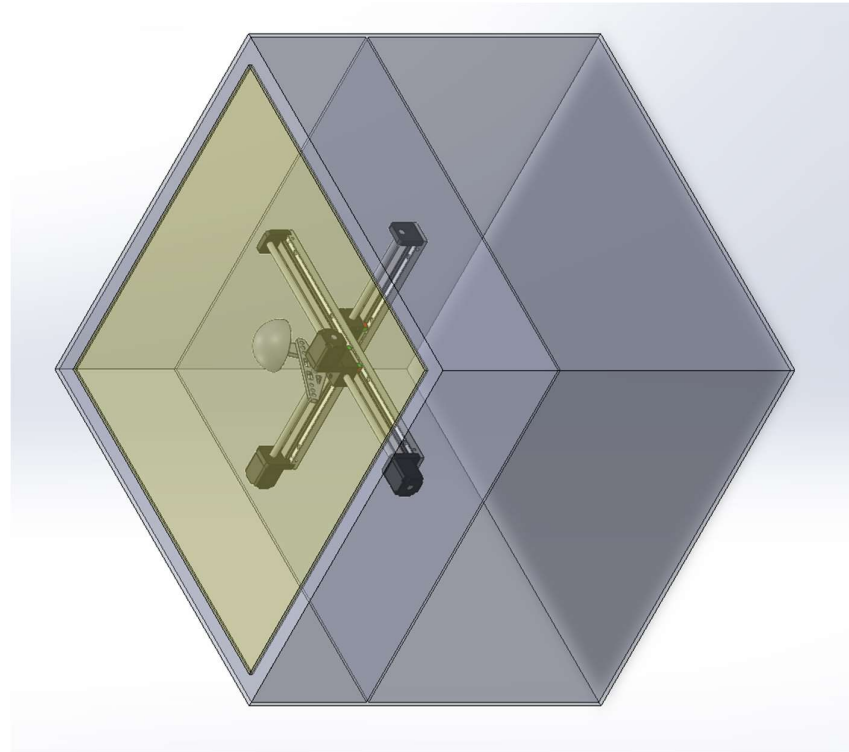


Fig 3.1

For the purpose of proofing the concept of aerodynamically adaptive bodies we have created a 3D geometry with a flexible face on one of its side shown in the yellow colour in the figure 3.1 the plane of actuation gives leverage to the body to change its shape in real time using real time data collected by the anemometer and processed by the on board computer.

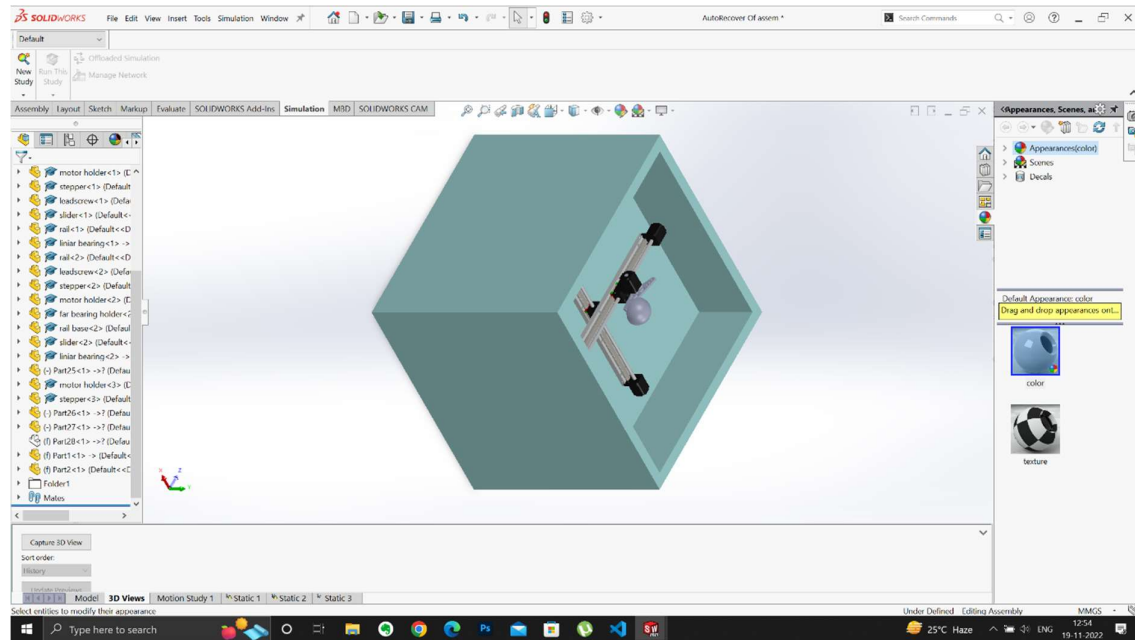
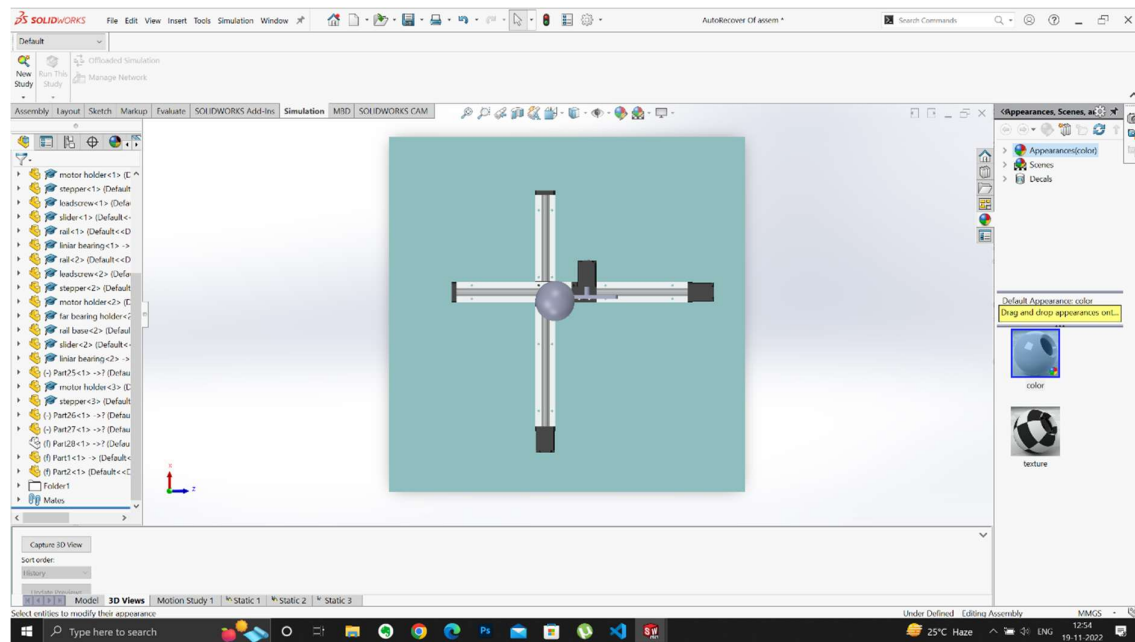


Fig 3.2

In the above figure 3.2 we can see the isometric view of the system where the internal mechanism is revealed which includes two lead screw operated actuators with stepper motor and a third plane actuator for deforming the flexible plane with desired amount of force and



displacement.

Fig 3.3

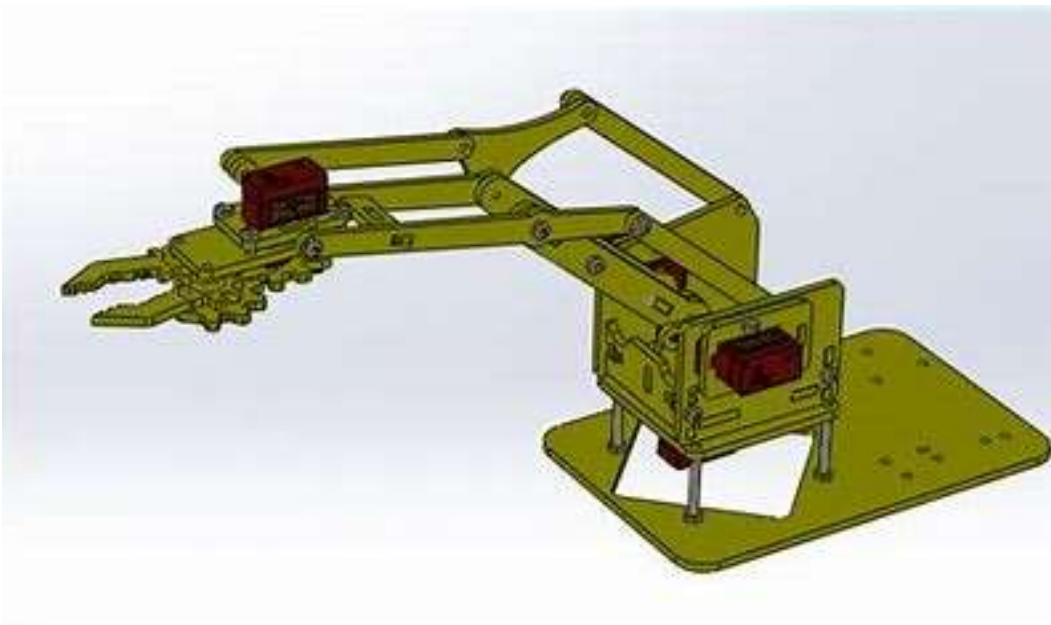


Fig 3.4

Although the geometry of the cube is simple, quite complex flow patterns are created in this flow configuration. The cube flow has been studied extensively both with CFD and numerically. In the present study, the control device consists of a deformable plane. This classical actuator is based on ideas of moving walls to reduce relative velocities at the flow boundaries in order to prevent or delay the flow separation. This method applied to a cube is numerically investigated in the present study and the flow control effects are checked and analysed.

### Numerical Set-up

The geometry of the cube and its placement inside the computational domain is shown in Fig. 1. The length of the side of the cube is  $W = 203$  mm and the rotating cylinders at two adjacent vertical surfaces have a diameter of  $Dr = 50.8$  mm. The wind tunnel has a span of  $5W$  and height of  $5W$ . The cube is placed at the middle of the span and  $1.5W$  height from the center to the floor. The center of the cube is located  $5.5W$  from the inlet and  $15.5W$  from the outlet. The inlet velocity,  $U_0$ , is  $5$  m/s, resulting in  $Re = 6.7 \times 10^4$  based on the height of the cube,  $W$ . Flows at two yaw angles of  $\theta = 0^\circ$  and  $\theta = 30^\circ$  were studied. In the simulations, a uniform and steady velocity is applied at the inlet and a homogeneous Neumann boundary condition is used at the outlet. The walls of the numerical wind tunnel are treated as slip walls. The surfaces of the cube are imposed to no-slip boundary conditions except on the control device (the shaded

surfaces in Fig. 1a) where a tangential velocity  $U_c = 2U_0$  is applied to simulate the rotating cylinders with direction of rotation indicated by the arrows in Fig. 1a. Note that the upper and lower surfaces of the cylinders do not rotate. In the present LES, the spatially implicitly filtered Navier–Stokes equations for the resolved scales are as follows:

$$\frac{\partial \bar{u}_i}{\partial t} + \frac{\partial \bar{u}_i \bar{u}_j}{\partial x_j} = -\frac{1}{\rho} \frac{\partial \bar{p}}{\partial x_i} + \nu \frac{\partial^2 \bar{u}_i}{\partial x_j \partial x_j} - \frac{\partial \tau_{ij}}{\partial x_j} \quad (1)$$

$$\frac{\partial \bar{u}_i}{\partial x_i} = 0. \quad (2)$$

The SGS stress tensor  $\tau_{ij} = u_i u_j - \bar{u}^- i \bar{u}^- j$  is modelled by the CSM, thus

$$\tau_{ij} = -2C\bar{\Delta}^2 |\bar{S}| \bar{S}_{ij} + \frac{1}{3} \tau_{kk} \delta_{ij} \quad (3)$$

where  $S^-_{ij}$  and  $|\bar{S}|$  are the velocity-strain tensor and the magnitude of the velocity gradient, respectively, i.e.

$$\bar{S}_{ij} = \frac{1}{2} \left( \frac{\partial \bar{u}_i}{\partial x_j} + \frac{\partial \bar{u}_j}{\partial x_i} \right); \quad |\bar{S}| = (2\bar{S}_{ij}\bar{S}_{ij})^{1/2}. \quad (4)$$

In the standard model, the model coefficient  $C$  in Eq. 3 is constant in the computational domain, and it does not satisfy a correct asymptotic behaviour to a wall. While in this, the model parameter  $C$  is dynamically calculated from the flow field based on the turbulence structures. It is determined as

$$C = C_{CSM}|F_{CS}|^{3/2}F_\Omega \quad (5)$$

with

$$C_{CSM} = \frac{1}{22}; \quad F_{CS} = \frac{Q}{E}; \quad F_\Omega = 1 - F_{CS} \quad (6)$$

$$Q = \frac{1}{2} (\bar{\Omega}_{ij}\bar{\Omega}_{ij} - \bar{S}_{ij}\bar{S}_{ij}) = -\frac{1}{2} \left( \frac{\partial \bar{u}_i}{\partial x_j} \right) \left( \frac{\partial \bar{u}_j}{\partial x_i} \right) \quad (7)$$

$$E = \frac{1}{2} (\bar{\Omega}_{ij}\bar{\Omega}_{ij} + \bar{S}_{ij}\bar{S}_{ij}) = \frac{1}{2} \left( \frac{\partial \bar{u}_i}{\partial x_j} \right)^2 \quad (8)$$

in the following figure we can see the meshing done for the study of computational fluid dynamics which gives exact wind flow patterns occurrences in the geometry at dynamic conditions

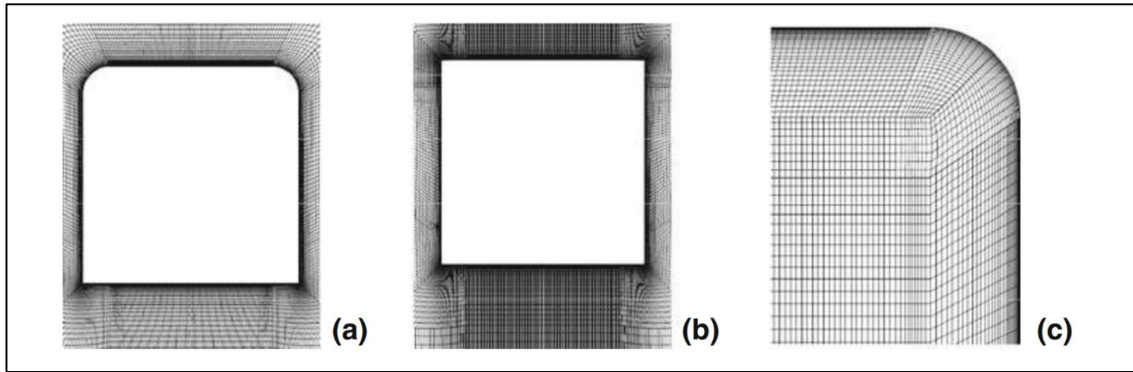


Fig 3.5

### **Case-1 0 ° Yaw angle.**

Figure 3.5 shows the comparison of the time-averaged streamlines between the non-deformed and deformed cases in the middle planes of the cube. The figures show that the flow structures are quite similar in the two cases. The main flow separations exist in the wake region and near the upper and lower surfaces of the cube. Figure 3.6 shows the iso-surface of the time-averaged streamwise velocity with a value of  $U = 0$  which can be viewed as a rough sketch of the structures of the separation bubbles. The sharp-edge separations on the upper and lower front edges result in much larger separation regions than the smooth-surface separation on the lateral sides of the cube. The results in Fig. 3.6 show that the separation regions are slightly changed

in the controlled case compared with those in the natural case. The main change is that the separation regions near the rotating cylinders are prevented due to MI which can be observed from the middle two figures (side view) in Fig. 3.6.

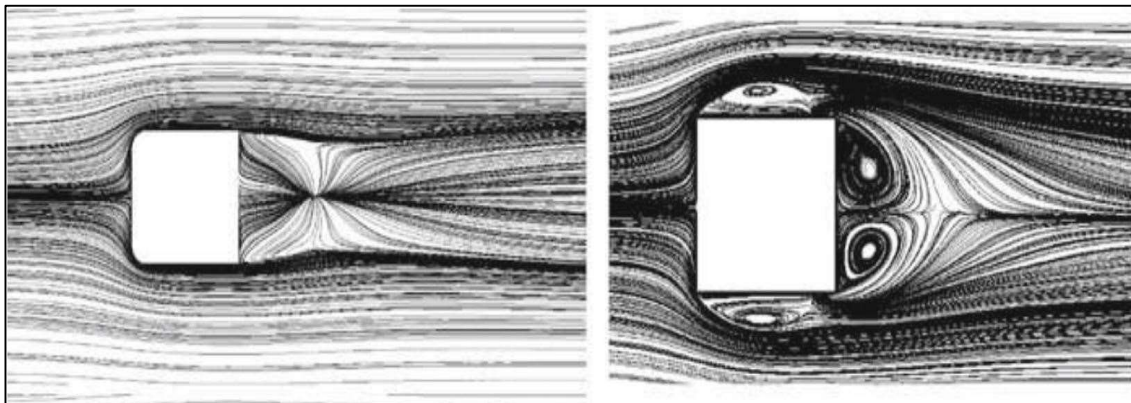


Fig 3.6

Fig. 3.7

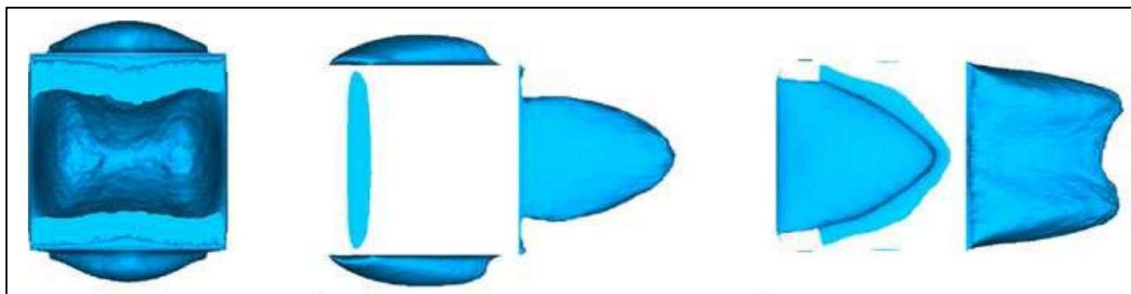


Fig 3.8

The following image 3.7 shows the velocity gradient across the geometry in the case of a body exposed to straight forward winds components of velocity are plotted in 3D space using Computational Analysis.

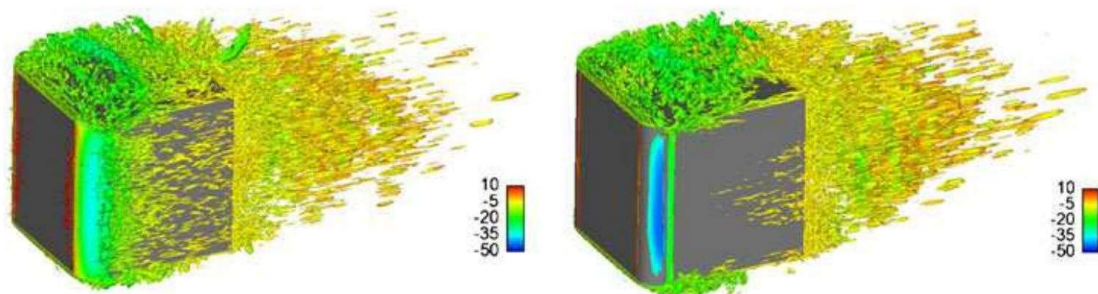


Fig 3.9

## Case-2 30° Yaw angle.

For the case of 30° yaw angle, the global parameters of drag, lift and yaw moment coefficients are compared in Table 3.1. The predicted drag coefficient has a difference of about 1.4 % and 3.4 % for the natural and the controlled case between the two meshes. The small differences mean that the mesh used in the simulations are fine enough for the LES study and the predictions are reliable. The predictions show that the drag is significantly reduced, with a reduction of about 44.1 % in the case of 30° yaw angle on the fine mesh M2, which is much larger than that in the 0 ° yaw angle case. The fluctuations of the drag, lift and yaw moment coefficients are quite small in both natural and controlled case. Furthermore, it seems that the fluctuations of these coefficients are depressed in the controlled case. At the same time, the control devices of the rotating cylinders affect the yaw moment significantly. The mean yaw moment coefficient is increased by about 50.5 %. It means that the mechanism make the cube easier to rotate along the z axis. Figure 3.8 shows the comparisons of the time-averaged streamlines between the natural and controlled case from top view in the middle plane of the cube. The figures show that the flow structures are changed a lot in the controlled case with the deformed surface. The large separation region on one lateral side of the cube is significantly depressed and the flow quickly attaches to the cube surface in the controlled case due to the moment injection.

**Table 2** Global parameters of the 30° yaw angle case: drag  $C_D$ , lift  $C_L$  and yaw moment  $C_Y$  coefficients

Case	$C_{D,ave}$	$C_{L,ave}$	$C_{Y,ave}$	$C_{D,rms}$	$C_{L,rms}$	$C_{Y,rms}$	$\Delta C_{D,ave}$	$\Delta C_{Y,ave}$
30°-NAT-M1	0.635	0.010	0.570	0.014	0.019	0.032	—	—
30°-CON-M1	0.338	-0.010	0.858	0.009	0.009	0.013	-46.8 %	50.5 %
30°-NAT-M2	0.626	-0.012	0.566	0.010	0.013	0.017	—	—
30°-CON-M2	0.350	-0.021	0.852	0.009	0.011	0.012	-44.1 %	50.5 %

NAT means the natural case and CON means the controlled case. M1 means the coarse mesh and M2 means the fine mesh.  $\Delta C$  is the difference between the values in the natural case and controlled case

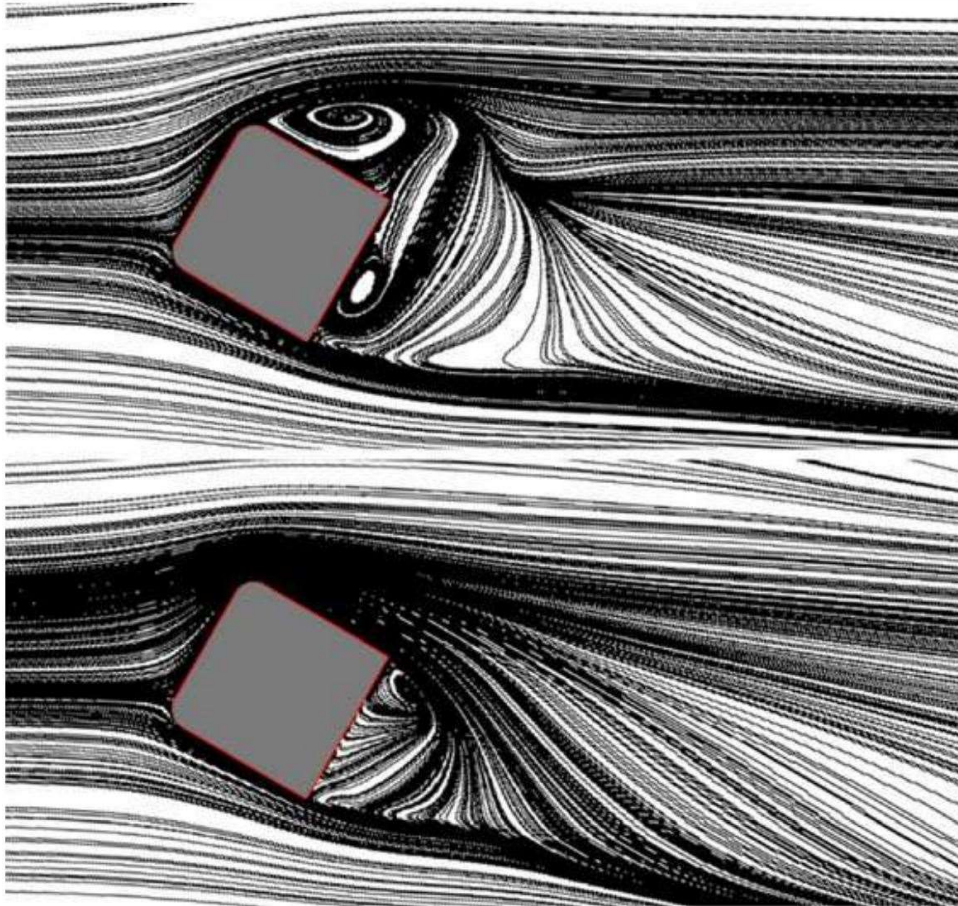


Fig 3.10

Figures 3.9 and 3.10 show the isosurface of the time-averaged streamwise velocity with a value of  $U = 0$  which can be viewed as a rough sketch of the structures of the separation bubble. The two rotating cylinders are distinguished by the numbering 1 and 2. In the natural case, the flow barely separates in the region around the mechanism along the lateral walls. There are four main separation regions, the first two (I and II) are located around the lower and upper surfaces of the cube, respectively, the third (III) is located along the vertical surface of the cube and the fourth (IV) is the wake region behind the cube.

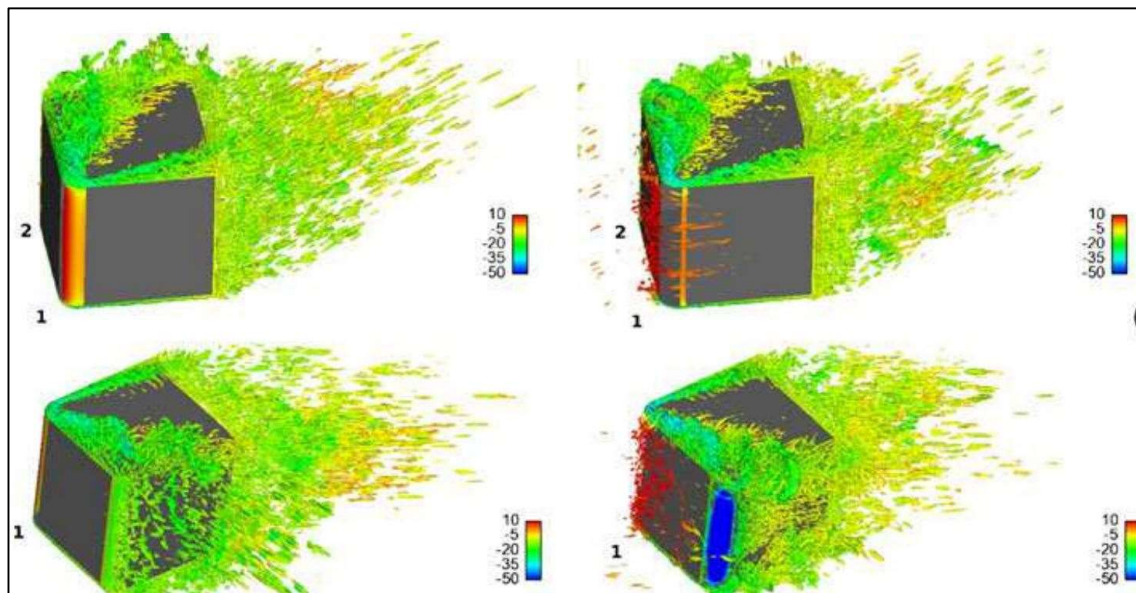


Fig 3.11

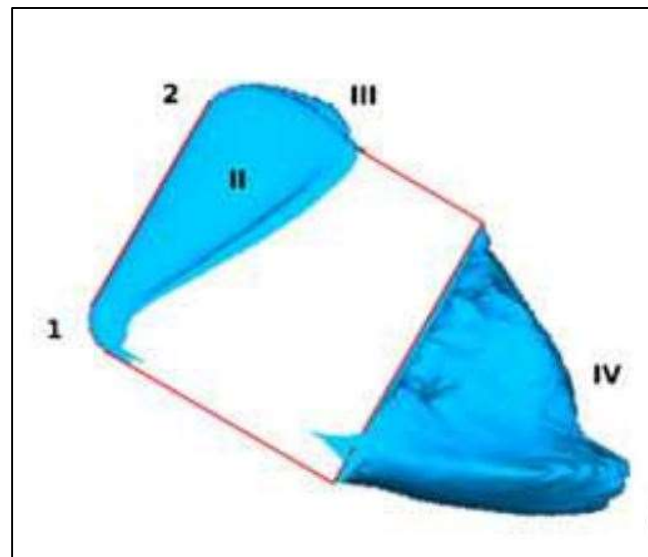


Fig 3.12

## **Conclusion.**

Two cases with a yaw angle of  $0^\circ$  and  $30^\circ$ , respectively, are studied. In the case of  $0^\circ$  yaw angle, a drag reduction of about 6.2 % is observed and about 44.1 % drag reduction is achieved in the  $30^\circ$  yaw angle case. Meanwhile, the yaw moment is increased about 50.5 % for the  $30^\circ$  yaw angle case. For both cases, the results demonstrate that this method can efficiently delay the boundary layer separation in the region where the momentum injection is applied, and thus reduces the drag. For the case of  $0^\circ$  yaw angle, the separation regions near the rotating cylinders disappear and the wake region is slightly changed. In the  $30^\circ$  yaw angle case, the flow field has changed significantly, i.e. the large flow separation at specific regions and in the wake can be drastically reduced. The study illustrates potential of using of this method for flow control problems.

The project on Adaptive Aerodynamic Bodies explores the concept of creating and using aerodynamic systems that can adapt and change shape in response to changing environmental conditions. The main aim of the project is to improve the overall performance, performance and safety by optimizing the aerodynamic components of various vehicles and models.

As a result of research and analysis, it has been determined that the modified aerodynamic body provides many benefits in many areas. The ability to dynamically adjust the shape and configuration of the surface will better control airflow, reduce drag and increase vehicle stability. This increases fuel efficiency, reduces emissions and improves overall performance. The project explores various technologies and techniques used to create aerodynamic body modifications, including body control systems, smart materials, and deformation models. This technology adjusts the aerodynamic shape of the fuselage in real time, providing the best performance in different missions. The integration of sensors, actuators and control algorithms facilitates smooth adjustment and ensures that the system responds well to changes in speed, wind direction and other important factors.

The report also examines the practical applications of modified aerodynamic bodies in the automotive, aerospace and renewable energy industries. The automotive industry can benefit from improved fuel efficiency and reduced emissions, while the aviation industry can improve aircraft manoeuvrability, stability and fuel consumption.

## Chapter 4: Mechanism and Working

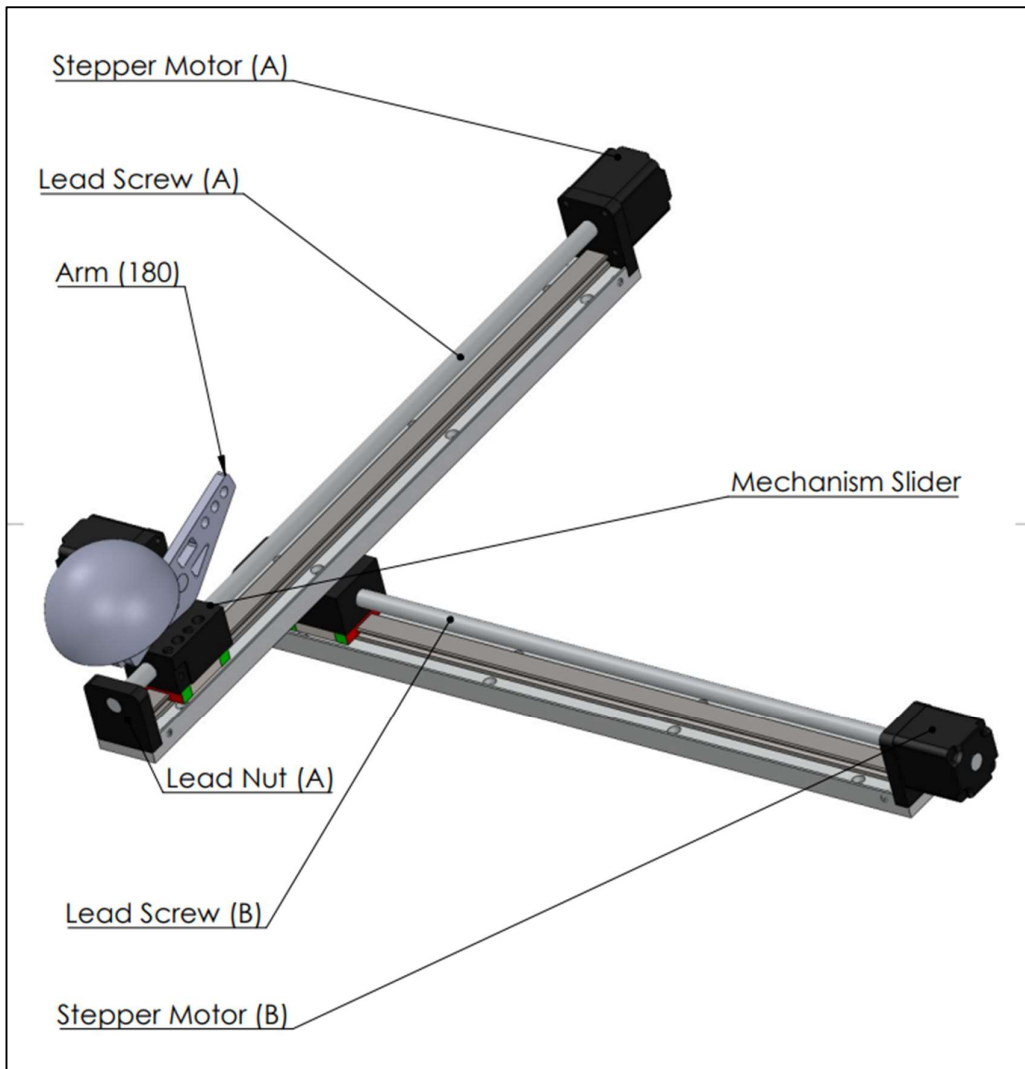


Fig 4.1

The Mechanism consists of the 3-Axis movement represented in pictorial format below. Placement of the mechanism is lateral and hence the much space is not required. Overall, it is a prototype for demonstration of the solution to the problem statement. This will give the overview of how the model will be in actual when implemented on Moving Bodies like Trucks, trailers, cars, busses, sports cars etc and stationary bodies such as Sky Scrappers, Electricity Transformers etc.

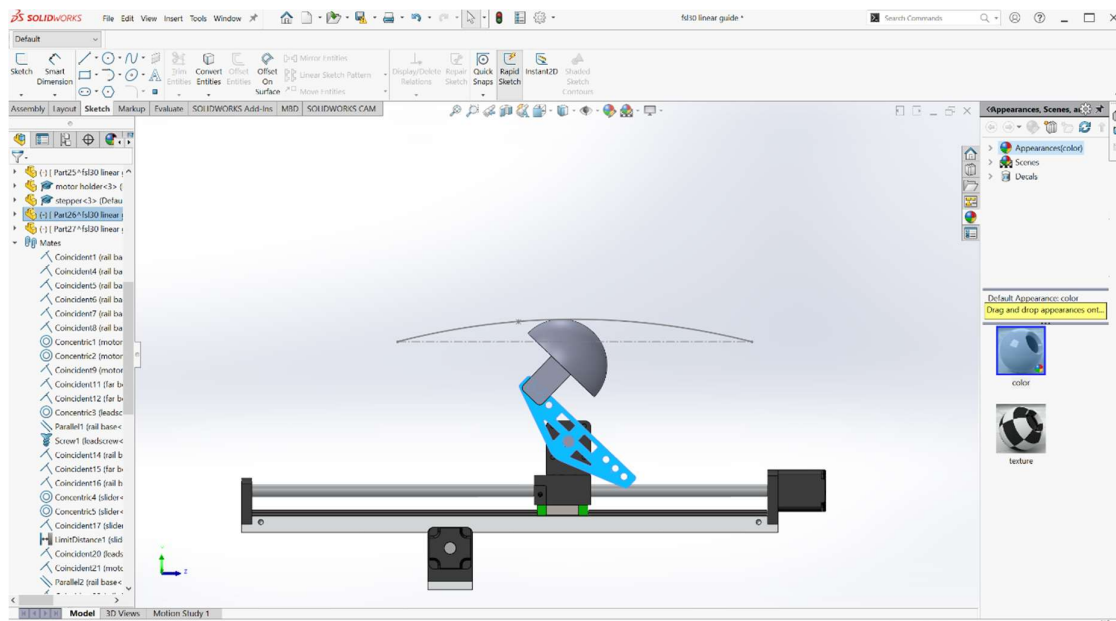


Fig 4.2

The above model depicts the system from the side view. This states the post actuated state in which we can see that the slider is intact at the principal point of operation and it provides the bulging effect to the material which we will be using. The material which we will use for that purpose will be the one with maximum elastic properties also with maximum strength.

Movement on Y-axis takes place with the help of lead screw actuated by the Stepper motor which will provide ultra-precision to the slider. The slider is mounted onto the lead screw of Y-axis and has capability to lock at the desired position with the help of threads which mesh with lead screw at the bottom part.

The Arm which is placed onto the slider is powered by the cube servo for stepwise increment and precision. This arm has the semi circular cup at the end which gives the final effect of bulging to the cloth / fiber / body part etc, wherever we implement our model.

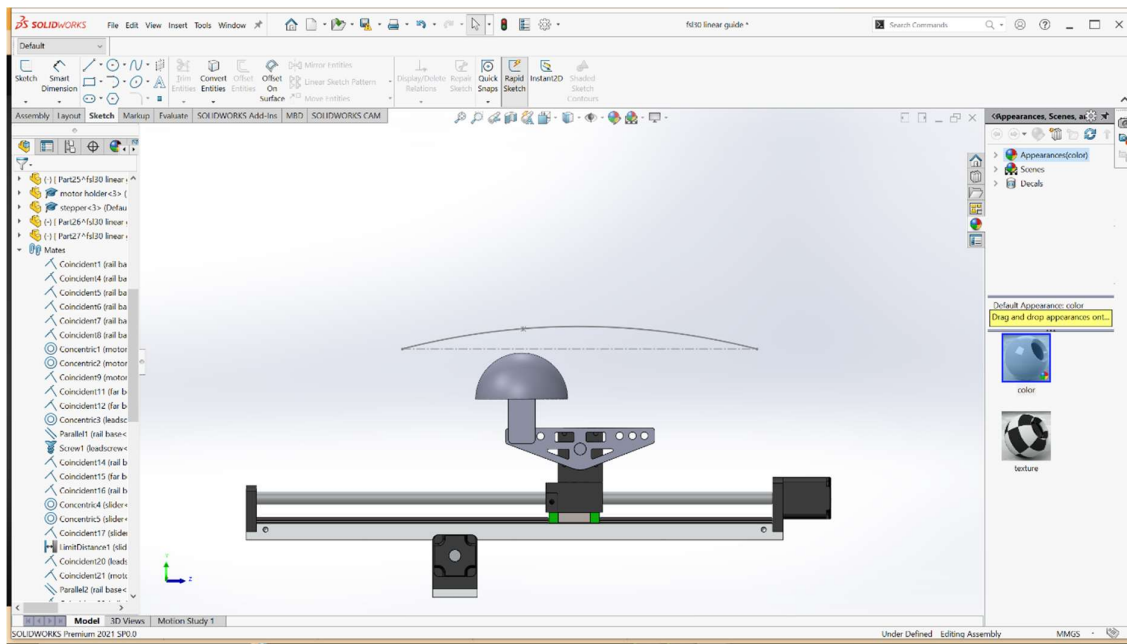


Fig 4.3

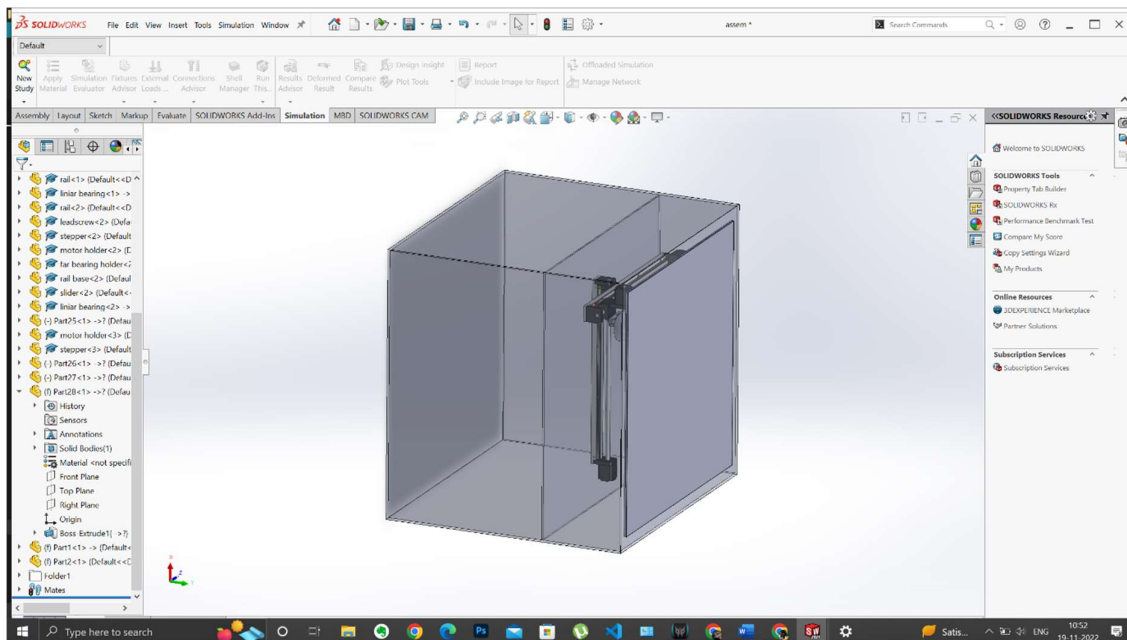


Fig 4.4

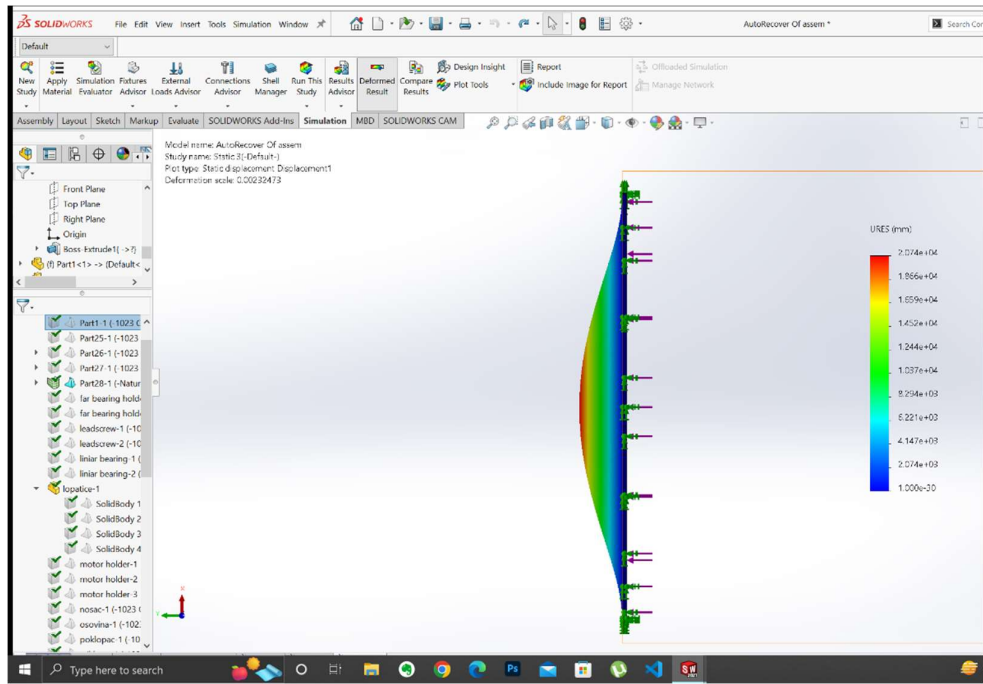


Fig 4.5

The figures 4.5 and 4.6 shows the defoemation pattern from the analysis. The actuated system will give the following results live extremity of deformation tends to increase as we go from end to centre. The panels may differ its material, physical or chemical properties but the deformation forces will be similar in all the types of the systems.

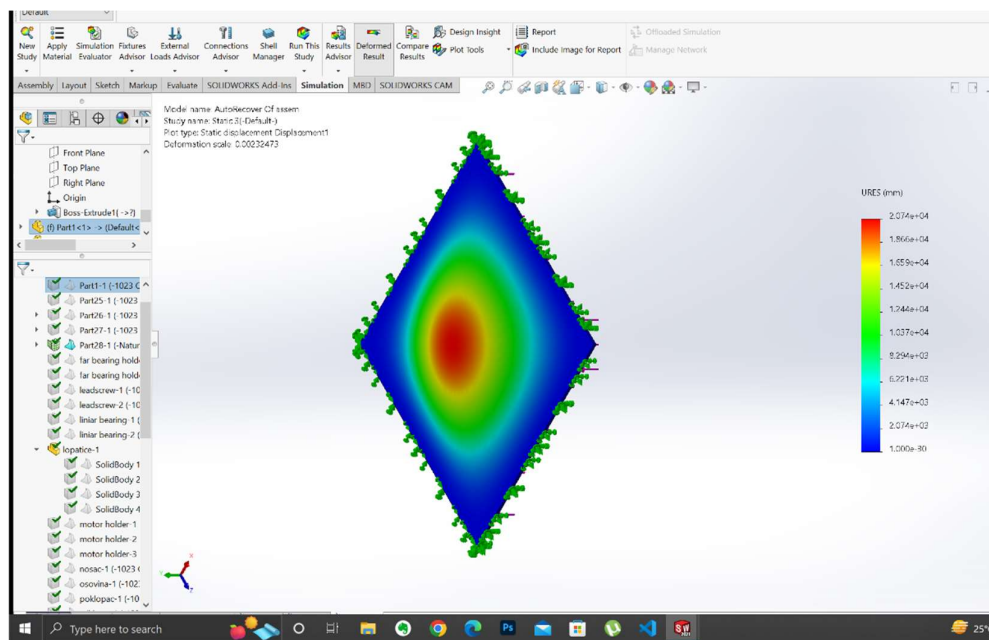


Fig 4.6

## Input Sensor:

The HCD6812 ultrasonic anemometer measures wind speed and direction using the difference in propagation time of ultrasonic waves in air. Compared with traditional mechanical anemometers, it has less wear, longer service life and faster speed. It can be widely used in urban environment monitoring, wind power generation, weather monitoring, bridges and tunnels, warships, aviation airports and other fields. No maintenance or field calibration required. Strong structure, strong corrosion resistance, not afraid of damage during installation and use. Flexible design, light and strong, easy to install and disassemble.

HCD6812 ultrasonic anemometer is used in urban environment monitoring, wind power generation, weather monitoring, bridges, tunnels, ships, flight airports, agricultural meteorology, hydrometeorology, energy environment, highway weather monitoring, etc. Can be used widely. fields. No maintenance or field calibration required.

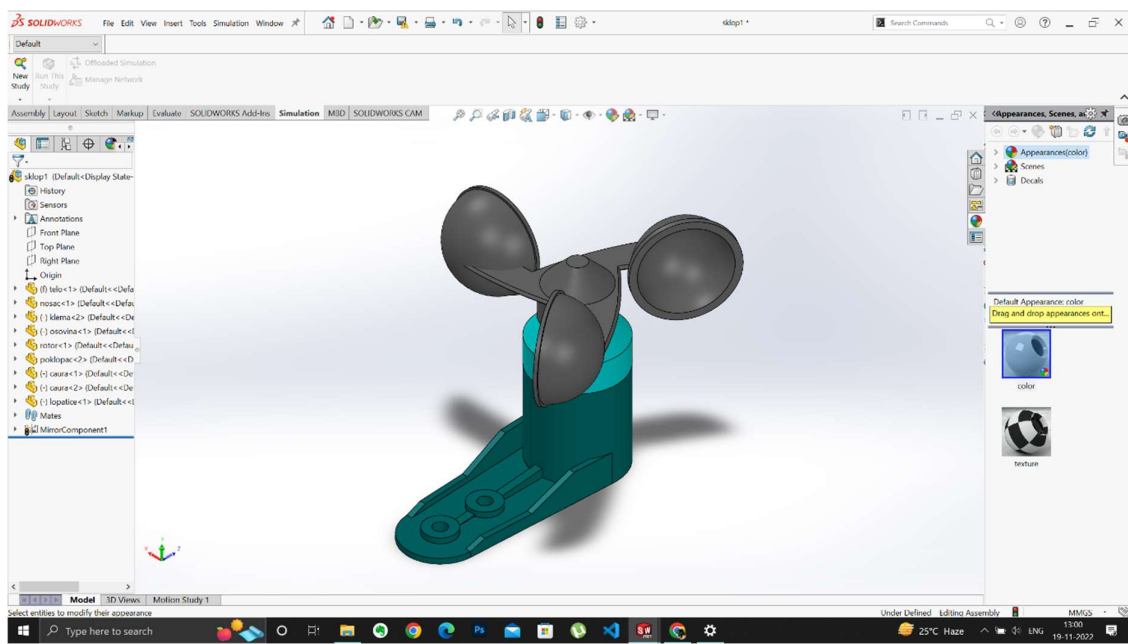


Fig 4.7

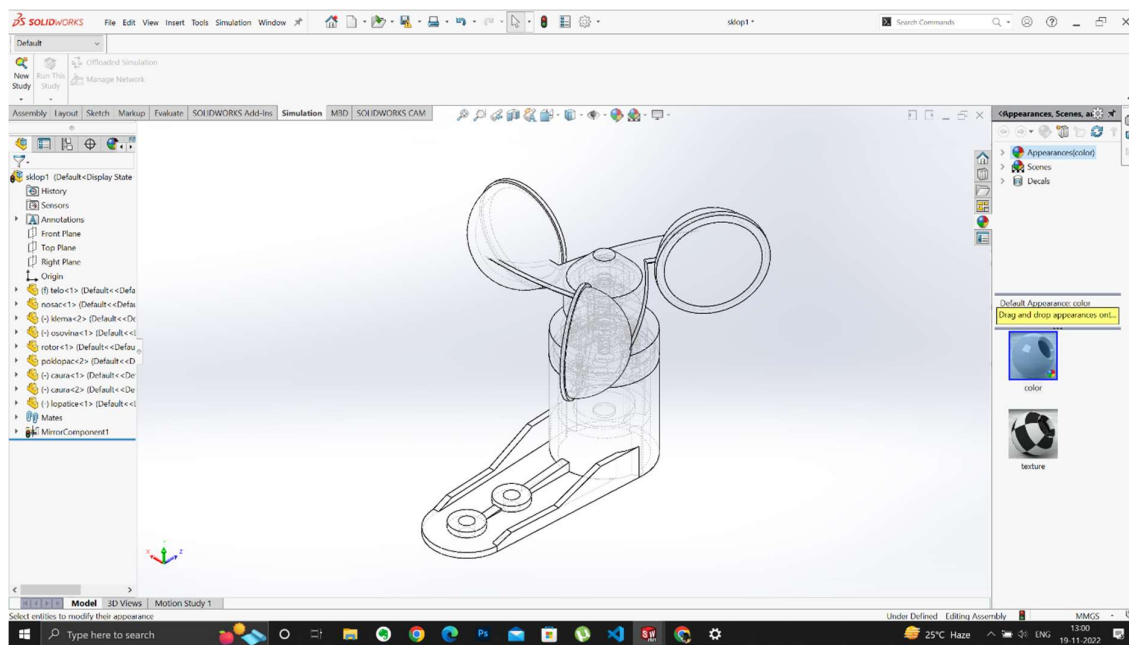


Fig 4.8

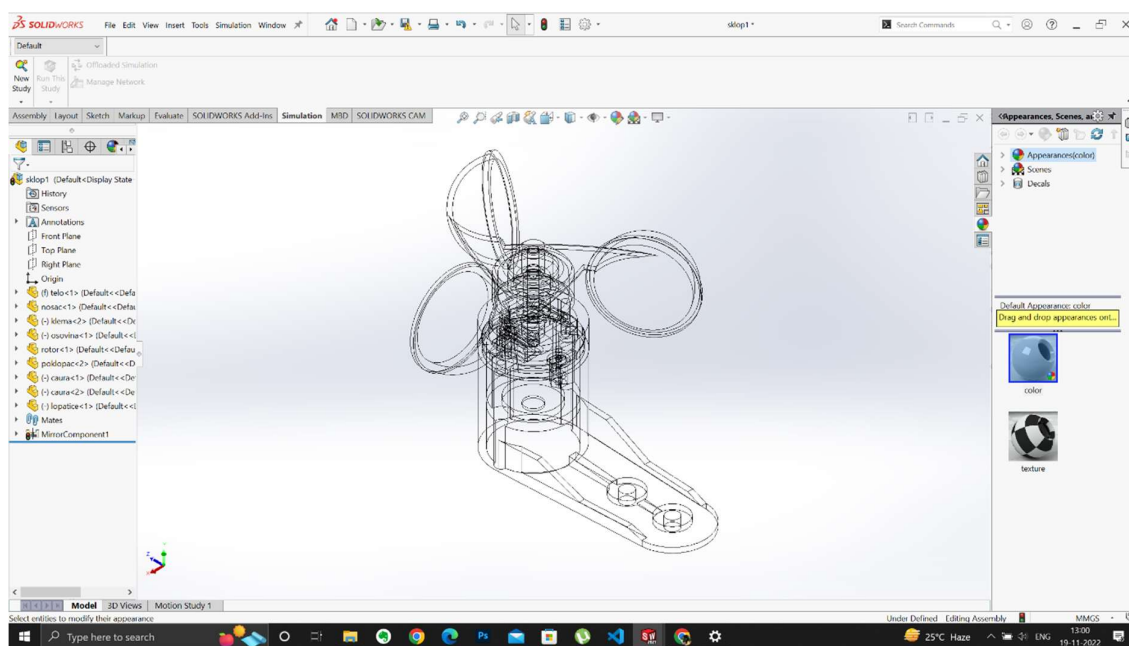


Fig 4.9

#### 4 Dof Arm Mechanism for 3 axis actuation :

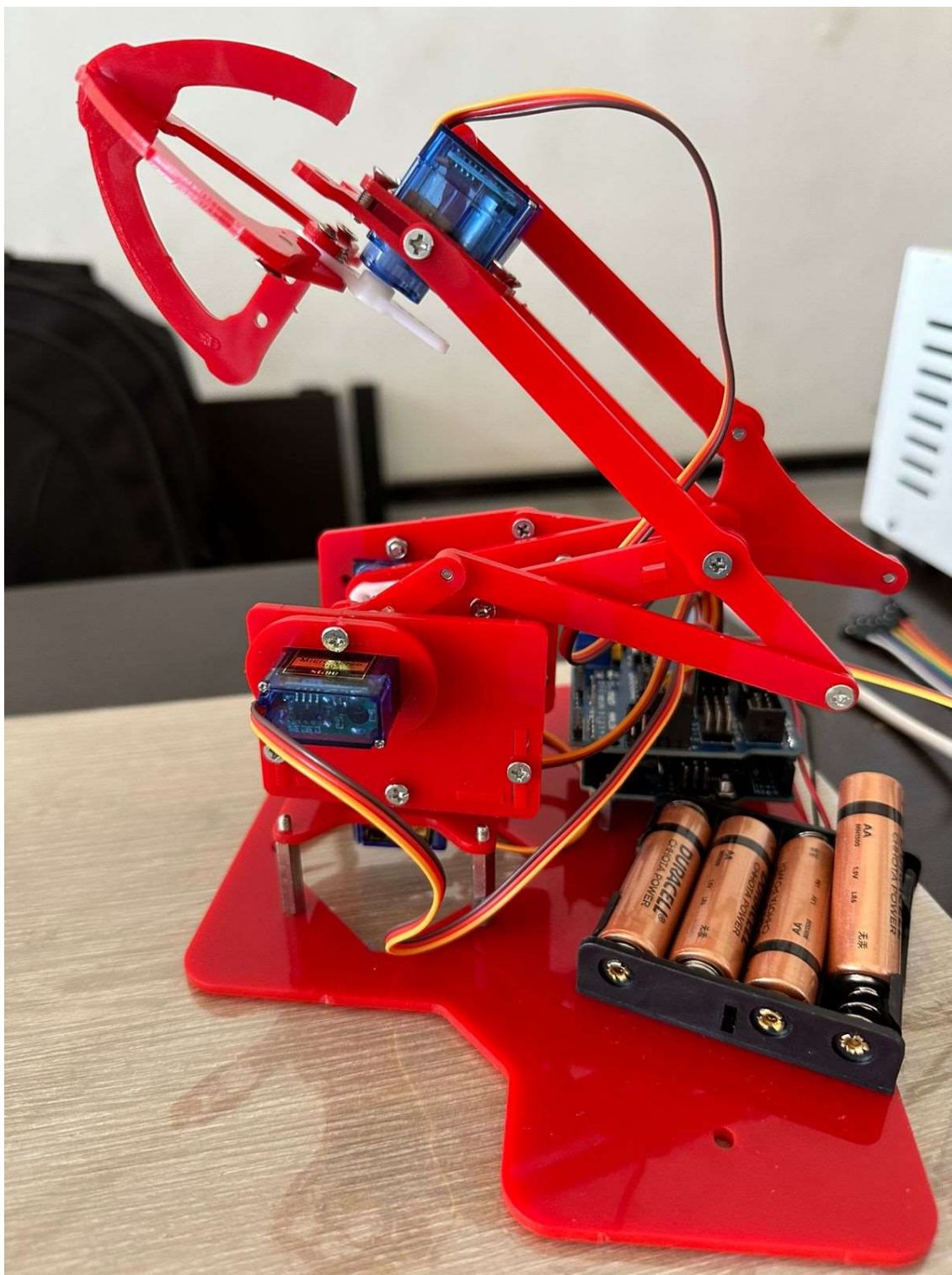


Fig 4.10

The custom-designed 4-DOF robotic arm is a versatile and precise manipulator capable of performing a wide range of tasks. It is specifically designed to meet the requirements of your project. The arm consists of four joints, each providing a degree of freedom, allowing it to move and position objects in a three-dimensional space.

- **Base Joint:** The base joint serves as the foundation of the robotic arm, enabling rotation along a vertical axis. This joint allows the arm to swivel and orient itself.
- **Shoulder Joint:** The shoulder joint connects the base joint to the upper arm and provides movement along the horizontal axis. It allows the arm to extend and retract, reaching different positions within its workspace.
- **Elbow Joint:** The elbow joint is located between the upper and lower arm segments. It enables the robotic arm to bend and straighten, providing vertical movement. This joint is essential for performing tasks that require reaching different heights.
- **Wrist Joint:** The wrist joint is the final joint in the arm, connecting the lower arm segment to the end effector. It provides both rotation and tilting motions, allowing the arm to manipulate objects with precision and dexterity.

The arm is constructed using lightweight and durable materials to ensure a balance between strength and agility. The joints are equipped with high-quality actuators or motors, such as servo motors or stepper motors, depending on the required level of accuracy and torque. To control the arm's movements, a combination of sensors, such as encoders and limit switches, are integrated into each joint. These sensors provide feedback on the position and orientation of the arm, enabling precise control and motion planning.

The arm can be controlled through a user-friendly interface, which can include buttons, joysticks, or even a graphical user interface (GUI). It can also be programmed to execute predefined sequences of movements or be controlled in real-time using external devices like sensors or cameras.

Additionally, the arm can be equipped with various end effectors or grippers, depending on the specific tasks required for your project. These end effectors can be interchangeable, allowing for flexibility and adaptability in different scenarios.

Overall, the custom-designed 4-DOF robotic arm offers a reliable and versatile solution for your project, with its ability to perform precise and controlled movements in multiple directions.

## Chapter 5: Components Used

### **Ultrasonic 2D Anemometer**



Fig. 5.1

The Ultrasonic 2D Anemometer is a compact ultrasonic wind speed and direction sensor. It is designed to simultaneously measure the two-dimensional horizontal component of wind speed and direction. The use of an ABS shell provides a lightweight and robust construction. With the built-in intelligent heating module, it can work normally even in extreme cold and freezing weather conditions.

The sensor's advanced ancillary electronics make it compact and reliable. Wind speed and direction sensor modules are available as external accessories. It can be integrated with our various ambient air quality monitoring stations, various monitors and the environmental weather station. The sensor module housing is a plug and play module. The sensor works with ultrasonic technology.

Sensor modules with no moving parts require little maintenance and provide accurate results over time. The module is robust and works with great stability even in extreme weather conditions. Additionally, the module exhibits excellent long-term stability and accuracy. All our products can be integrated with this sensor module. This module is therefore ideal for traffic control, meteorology, oil rigs, marine applications, industrial automation, wind turbines and weather stations.

Technical specifications of the sensor are as follows:

	Wind Speed	Wind Direction
Measurement Range	0-40m/s	0-359°
Sensor Life	2 years	2 years
Minimum detection limit	0.1 m/s	1°
Working Principle	Ultrasonic	Ultrasonic

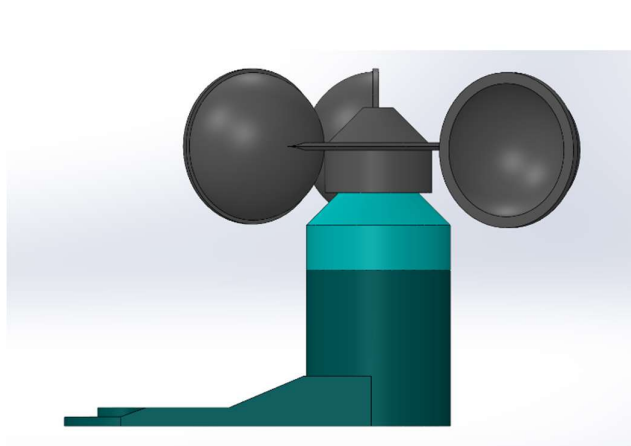


Fig 5.2

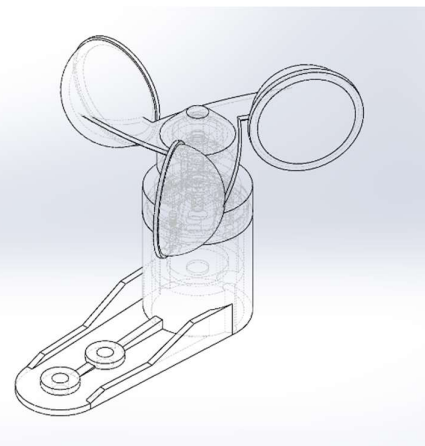


Fig 5.3

The custom-designed anemometer for this project is a compact and efficient device that accurately measures wind speed and direction. It is specifically tailored to meet the requirements of your project and offers the following features:

- **Sensor Technology:** The anemometer incorporates advanced sensor technology, such as ultrasonic anemometry or cup anemometry, to capture wind speed and direction data with high precision. The choice of sensor technology can be determined based on the specific needs and environmental conditions of your project.
- **Compact Design:** The anemometer is designed to be compact and lightweight, allowing for easy installation and portability. Its small form factor ensures minimal interference with the airflow and enables deployment in various locations, including remote or hard-to-reach areas.

- **Weatherproof Enclosure:** The anemometer is housed in a rugged and weatherproof enclosure, ensuring protection against harsh environmental conditions, including rain, snow, and extreme temperatures. This feature allows for reliable operation in outdoor settings over extended periods.
- **Mounting Options:** The anemometer offers versatile mounting options to accommodate different installation requirements. It may include brackets, clamps, or mounting plates that allow for secure attachment to poles, masts, or other structures. The mounting mechanism ensures stability and optimal positioning for accurate wind measurement.
- **Data Acquisition and Processing:** The anemometer incorporates a data acquisition system responsible for collecting, processing, and storing wind speed and direction data. This system can include microcontrollers, memory storage, and signal conditioning circuitry to ensure accurate and reliable measurements.
- **Power Supply:** The anemometer is designed to operate with various power sources, such as batteries, solar panels, or external power connections. The power supply is selected based on the project's specific needs, ensuring continuous and reliable operation.
- **Output and Connectivity:** The anemometer provides output options to interface with other systems or devices. It may include communication interfaces like USB, RS-232, RS-485, or wireless connectivity for seamless integration with data loggers, microcontrollers, or computer systems. These interfaces enable the transfer of wind data for further analysis and visualization.
- **Calibration and Accuracy:** The anemometer undergoes rigorous calibration procedures to ensure accurate and reliable measurements. Calibration can be performed using reference instruments or wind tunnels to verify the precision of wind speed and direction readings. This ensures that the anemometer provides consistent and trustworthy data for your project.

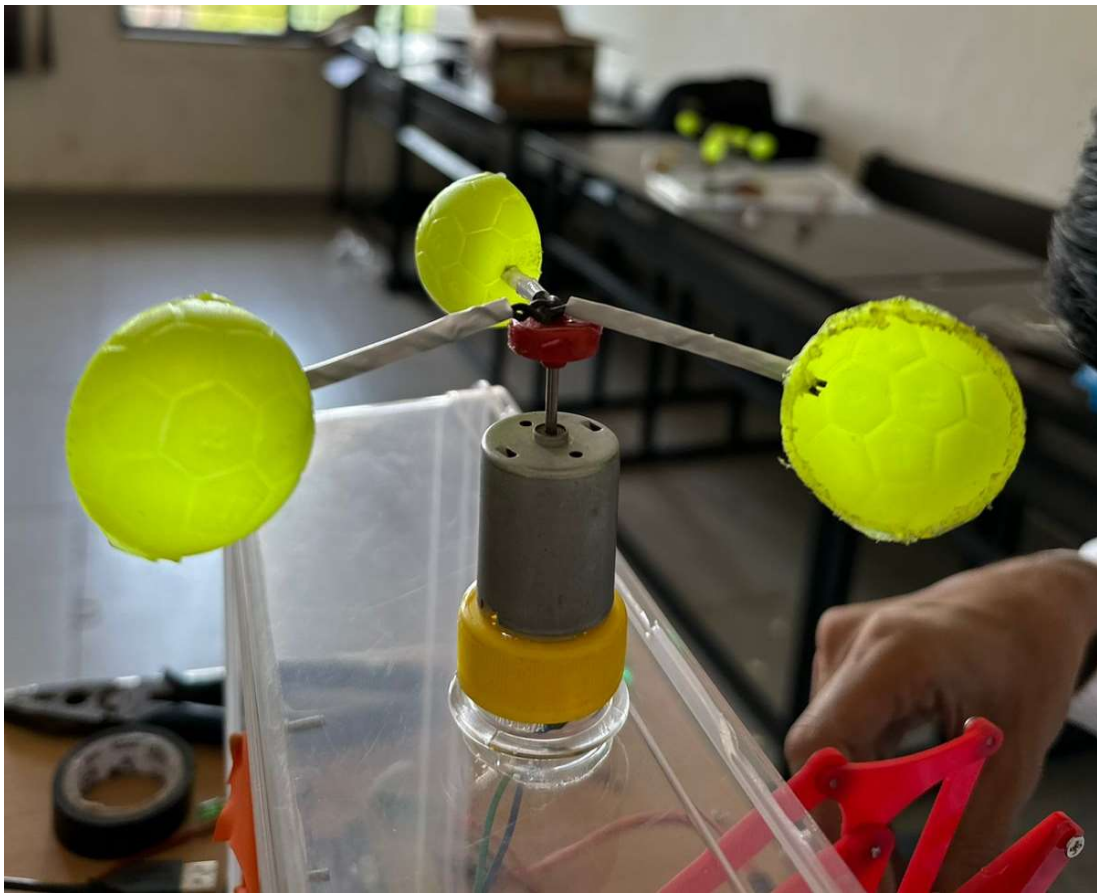


Fig 5.4

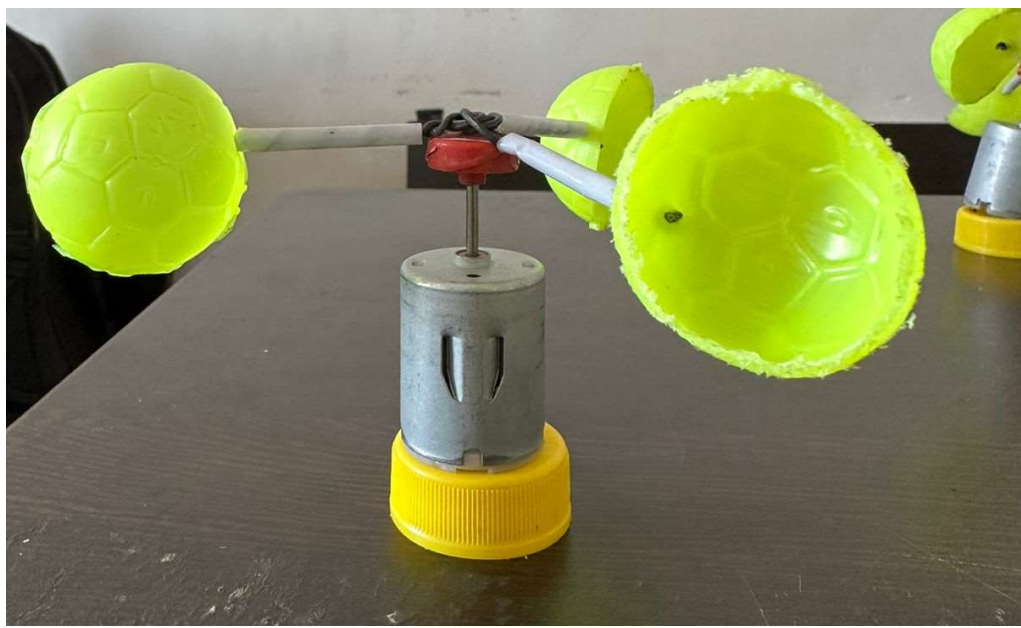


Fig 5.5

By utilizing this custom-designed anemometer, your project can obtain precise wind speed and direction measurements for applications such as weather monitoring, environmental research, or renewable energy analysis. Its tailored features and reliable performance make it a valuable tool for capturing critical wind data specific to your project's requirements.

## **Laser Cut Mounting Plate for ARM**

The plate is designed in the CAD software with reference to the topological geometry of the arm. Further it went through stress, strain and deformation analysis with ANSYS. Laser cutting was best suited as the manufacturing method for the plate and hence the work was outsourced at the local vendor of laser cutting. Laser cutting is the process of cutting, scoring, engraving, or otherwise altering physical materials using a laser. Although it may sound futuristic, laser cutting is a technology that has been with us for decades. Like many innovations, it was initially limited in scope, but has since been adopted with great enthusiasm across a great many industries.

Laser cutting, of course, begins with a laser beam. The beam is focused until it is strong enough for the task at hand, such as cutting metal, human tissue, or cardboard. A computer program controls the laser itself and determines the pattern the laser beam cuts. Once started, the laser follows a pre-programmed guide to complete the job.

Depending on the material and the desired result, the laser beam is moved and the focal length is changed. This allows you to reach different depths and cut different layers of material. In metal, this is useful for techniques such as engraving. However, in other applications such as medical, the pinpoint accuracy enables cutting of medical devices.

## **Servo SG90 Motor**

Tiny and lightweight with high output power. Servo can rotate approximately 180 degrees (90 in each direction), and works just like the standard kinds but smaller. You can use any servo code, hardware or library to control these servos. Good for beginners who want to make stuff move without building a motor controller with feedback & gear box, especially since it will fit in small places. It comes with 3 horns (arms) and hardware.

G15 Cube Servo is a modular smart serial servo which incorporates gear reducer, precision high torque DC motor and control circuitry with networking functionality. It is made with high quality engineering plastic to provide high necessary strength and is able to sustain high external force up to 15 kg.cm. holding torque. G15 provides 360° endless electrical

rotation by using potentiometer to lead itself to solve some application such as to motorize a mobile robot. G15 also has LED indicator to show the status of the servo.

The unique cubical design of G15 gives the highest flexibility in robotics model construction. By incorporating slidable slots and latches, G15 are able to eliminate the screws and nuts during the construction. This patented joining method enable user to connect a G15 to another G15 even easier and faster without any single screw. The robotic servo has never been this flexible before its existence.

The field of aerodynamics plays an important role in the design and operation of many vehicles, models and systems. Traditionally, the aerodynamic shape and configuration have been optimized for specific operating conditions, resulting in reduced overall performance. However, recent advances in data, sensors and technology have led to the development of modified aerodynamic bodies that can change their shape and behavioural set in response to changes. These modified systems have the potential to transform performance, mobility and safety in a wide range of applications, from aircraft and cars to wind turbines and toys.

## **Features:**

- Modular type robotic servo
- Cubical outlook and centre output shaft to give highest flexibility during robotic model construction
- Five slide-able slots in different orientation
- Screw-less mounting method
- 360° endless electrical rotation (1088 steps)
- Daisy chain connection wiring among the G15 cube servos (each G15 cube servo has its own unique ID)
- Serial communication, Half-duplex Asynchronous (max speed up to 500k bps), TTL level, command packet
- Rotation speed or time to reach the desired position can be set
- Able to feedback its angular position, angular speed, current load, temperature and supply voltage
- Auto shutdown if overload, supply voltage error or high temperature is detected (user define the value)
-

## Specifications:

- Weight: 9 g
- Dimension: 22.2 x 11.8 x 31 mm approx.
- Stall torque: 1.8 kgf·cm
- Operating speed: 0.1 s/60 degree
- Operating voltage: 4.8 V (~5V)
- Dead band width: 10  $\mu$ s

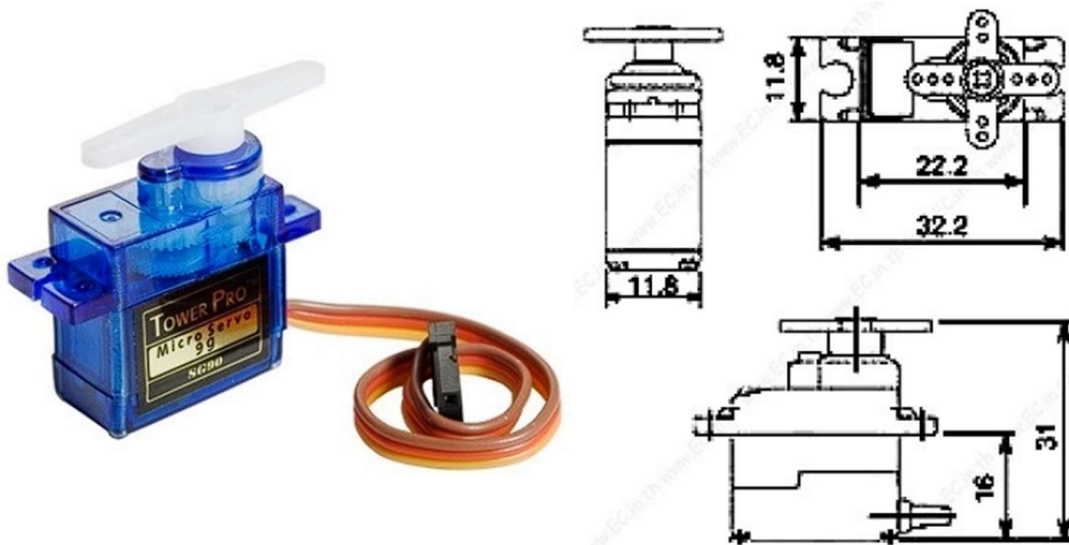


Fig 5.6



Fig 5.7

## Microcontroller

We chose the Arduino Uno microcontroller board for actuating the 4-degree-of-freedom (DOF) robotic arm due to several compelling reasons:

- 1. Versatility and Community Support:** Arduino Uno is a widely popular and versatile microcontroller board, offering a broad range of capabilities and compatibility with various sensors, actuators, and components. Its large user community ensures ample online resources, tutorials, and forums where I can seek assistance and share knowledge during the development process.
- 2. Ease of Use and Programming:** Arduino Uno provides a beginner-friendly environment for programming and prototyping. Its user-friendly integrated development environment (IDE) simplifies the coding process, allowing me to quickly develop and modify the control algorithms for the robotic arm. The simplicity of the Arduino programming language, which is based on C/C++, enables rapid prototyping and iterative development.
- 3. Ample I/O Pins:** The Arduino Uno board offers a sufficient number of digital and analog input/output (I/O) pins to connect and control the various components of the robotic arm. These pins can be used to interface with servo motors, sensors, buttons, and other peripherals, ensuring seamless integration and control of the arm's actuation.
- 4. PWM Support:** Pulse-width modulation (PWM) is essential for precise control of servo motors, which are commonly used in robotic arm applications. Arduino Uno has built-in PWM capabilities, allowing me to generate the required control signals with ease. This feature is crucial for accurately positioning the robotic arm and achieving smooth and controlled movements.
- 5. Cost-Effectiveness:** Arduino Uno offers a cost-effective solution for controlling the robotic arm. Its affordability compared to other microcontroller platforms or specialized control boards makes it an attractive option, especially for projects with budget constraints or educational purposes.
- 6. Expandability and Upgradability:** The modular nature of Arduino Uno enables easy expansion and upgradability. I can add additional shields or modules, such as motor driver boards, wireless communication modules, or sensors, to enhance the functionality and capabilities of the robotic arm as the project progresses.

**7. Educational Value:** Arduino Uno is widely used in educational settings to introduce students to the concepts of robotics and programming. By utilizing Arduino Uno for the robotic arm, I can leverage its educational value and access a wealth of educational materials and curriculum resources designed for Arduino-based projects.

Considering these factors, Arduino Uno provides a suitable platform for actuating the 4-DOF robotic arm, combining ease of use, flexibility, community support, and cost-effectiveness. Its extensive capabilities and compatibility make it an ideal choice for controlling and programming the robotic arm's movements and interactions.



Fig 5.6



Fig 5.7

The Arduino UNO R3 is the perfect board to get familiar with electronics and coding. This versatile microcontroller is equipped with the well-known ATmega328P and the ATMega16U2 Processor.

This board will give you a great first experience within the world of Arduino.

## Features

- **ATMega328P Processor**
- **Memory**
  - AVR CPU at up to 16 MHz 32KB Flash
  - 2KB SRAM
  - 1KB EEPROM
- **Security**
  - Power On Reset (POR)
  - Brown Out Detection (BOD)
- **Peripherals**
  - 2x 8-bit Timer/Counter with a dedicated period register and compare channels
  - 1x 16-bit Timer/Counter with a dedicated period register, input capture and compare channels
  - 1x USART with fractional baud rate generator and start-of-frame detection
  - 1x controller/peripheral Serial Peripheral Interface (SPI)
  - 1x Dual mode controller/peripheral I2C
  - 1x Analog Comparator (AC) with a scalable reference input
  - Watchdog Timer with separate on-chip oscillator
  - Six PWM channels
  - Interrupt and wake-up on pin change
- **ATMega16U2 Processor**
  - 8-bit AVR® RISC-based microcontroller
- **Memory**
  - 16 KB ISP Flash
  - 512B EEPROM
  - 512B SRAM

- debugWIRE interface for on-chip debugging and programming
- Power
  - 2.7-5.5 volts

UNO board is the main product of Arduino. Whether you're new to the world of electronics or using UNO as a tool for educational or business-related projects.

**First Touch with Electronics:** If this is your first project in the world of coding and electronics, start with our most used and best reference board; Arduino Uno. Equipped with the famous ATmega328P processor, 14 digital input/output pins, 6 analog inputs, USB connection, ICSP header and reset button. This board contains everything you need for your first Arduino experience.

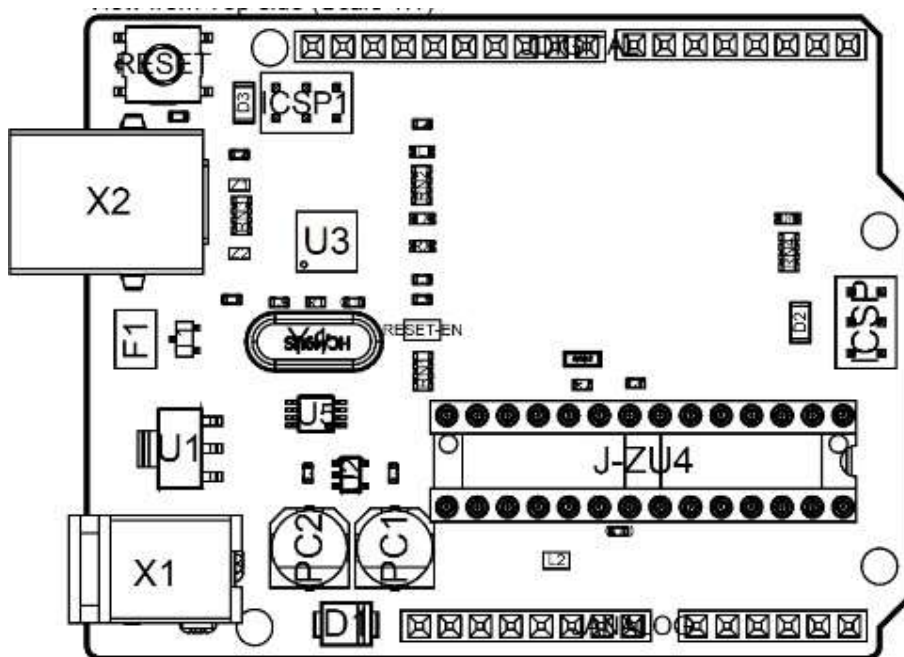


Fig. 5.8

Ref.	Description	Ref.	Description
X1	Power jack 2.1x5.5mm	U1	SPX1117M3-L-5 Regulator
X2	USB B Connector	U3	ATMEGA16U2 Module
PC1	EEE-1EA470WP 25V SMD Capacitor	U5	LMV358LIST-A.9 IC
PC2	EEE-1EA470WP 25V SMD Capacitor	F1	Chip Capacitor, High Density
D1	CGR4007-G Rectifier	ICSP	Pin header connector (through hole 6)
J-ZU4	ATMEGA328P Module	ICSP1	Pin header connector (through hole 6)
Y1	ECS-160-20-4X-DU Oscillator		

## Bluetooth Module [HS05]

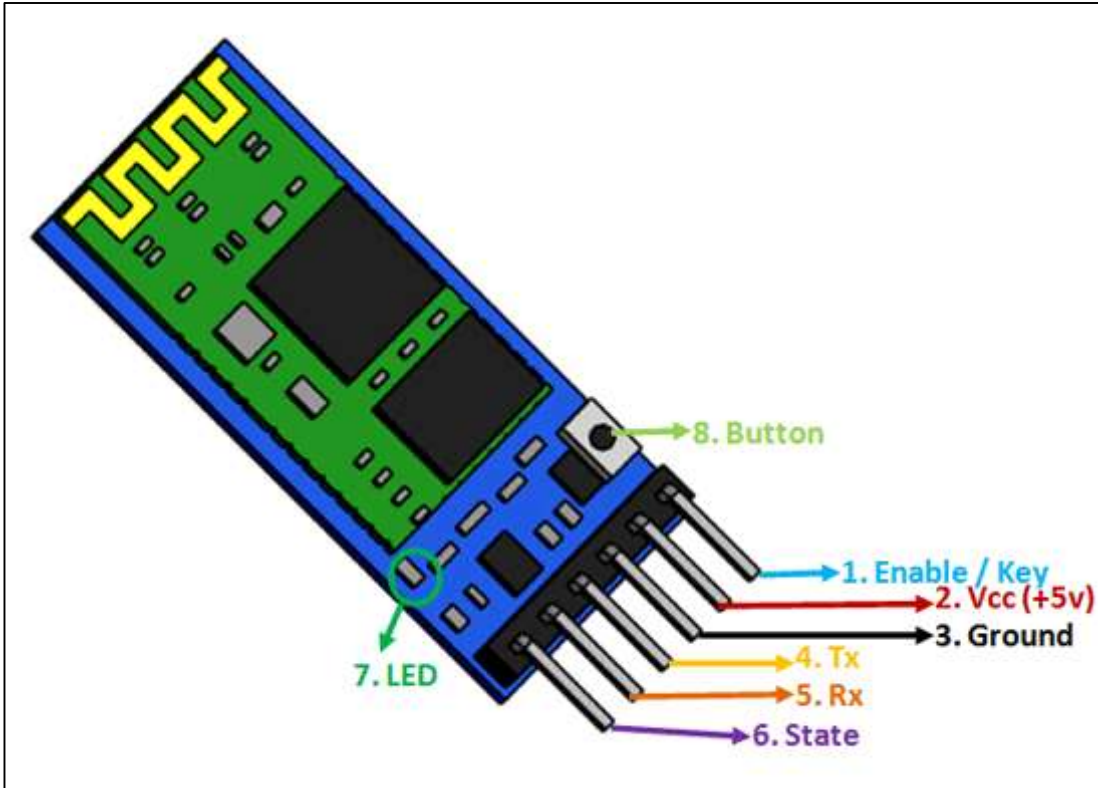
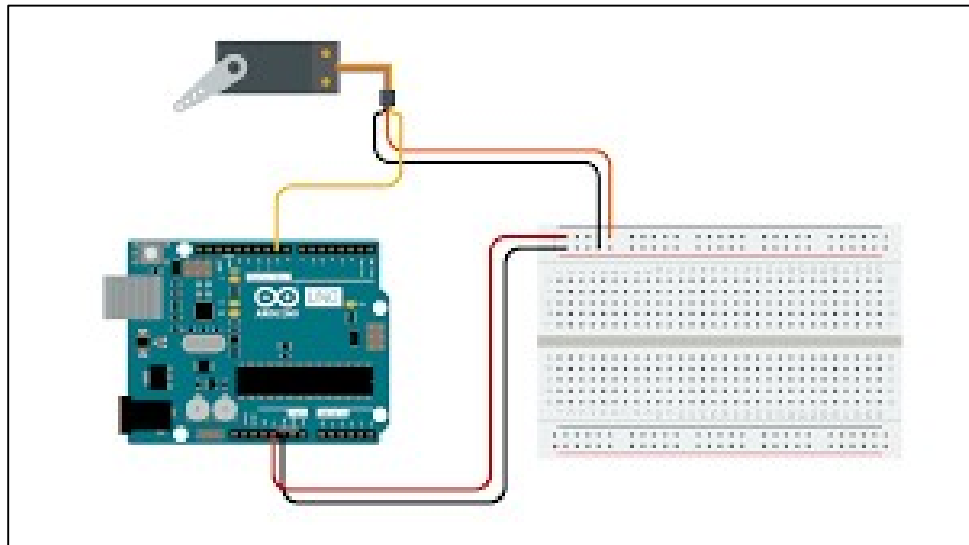


Fig. 5.9

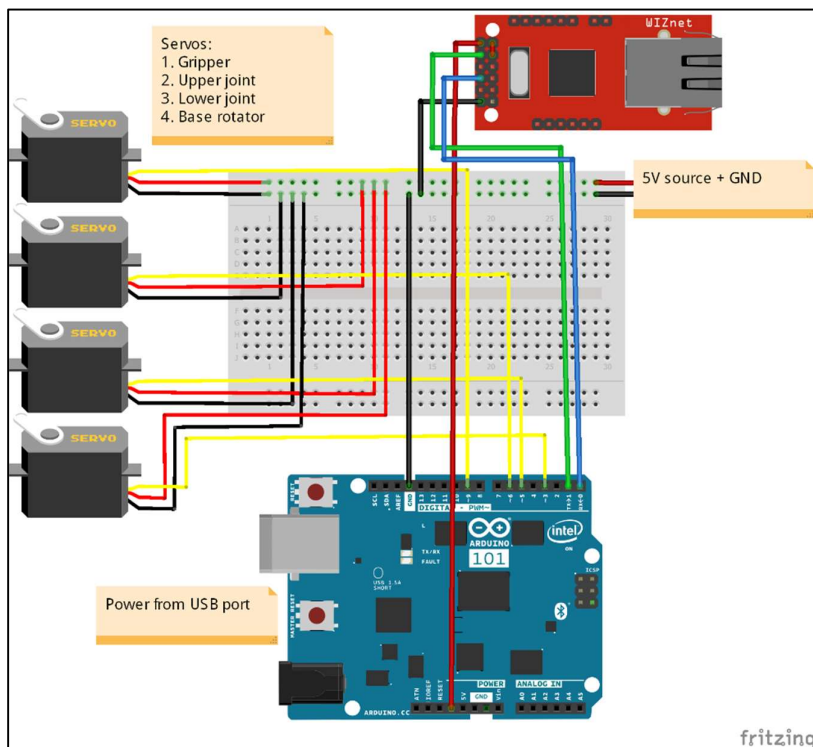
The HC-05 is a popular module that adds bidirectional (full duplex) wireless capability to your project. You can use this model to communicate between two microcontrollers like Arduino or with a Bluetooth device like a phone or laptop. Many Android apps are already available that make the process very easy. The module communicates via USART at 9600 baud so it can easily interface with any microcontroller that uses USART. We can also set the values of the module using the mode command.

Therefore, if you are looking for a wireless module that can transfer data from your computer or mobile phone to the microcontroller and vice versa, this module will be the right choice for you. But don't expect this module to change many things like pictures or music; you might want to look into the CSR8645 module for this.

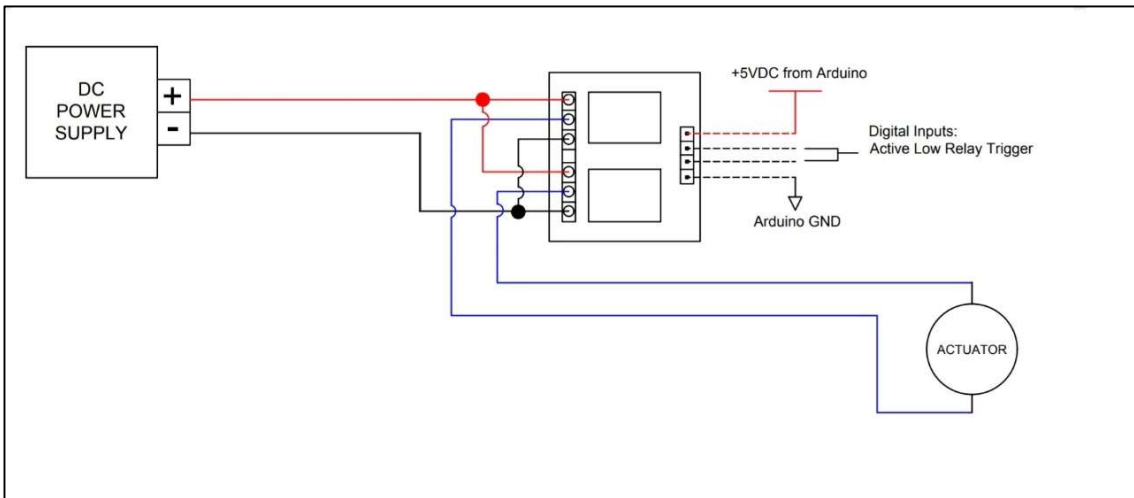
## Schematic / Circuit



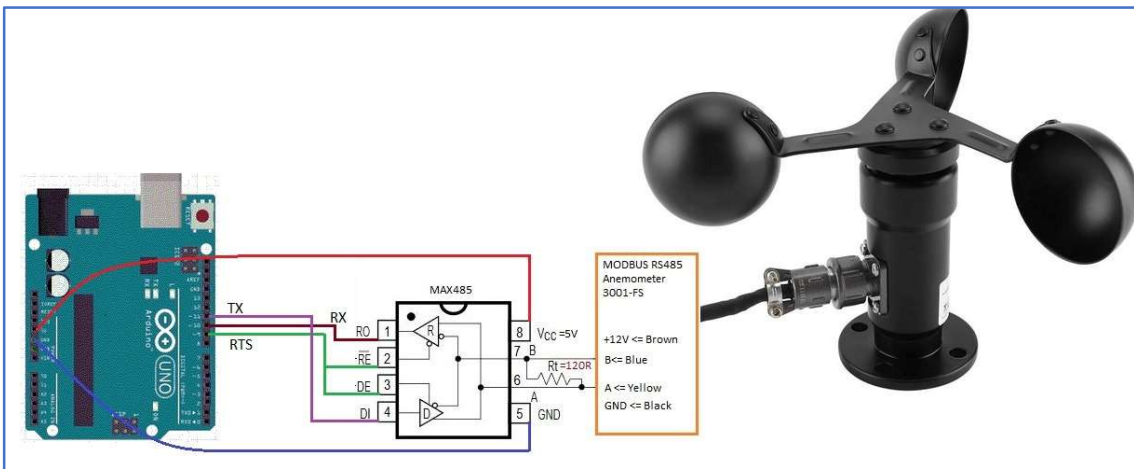
Circuit 1 : Servo – Arm Mechanism



Circuit 2 : Arm Controller Mechanism

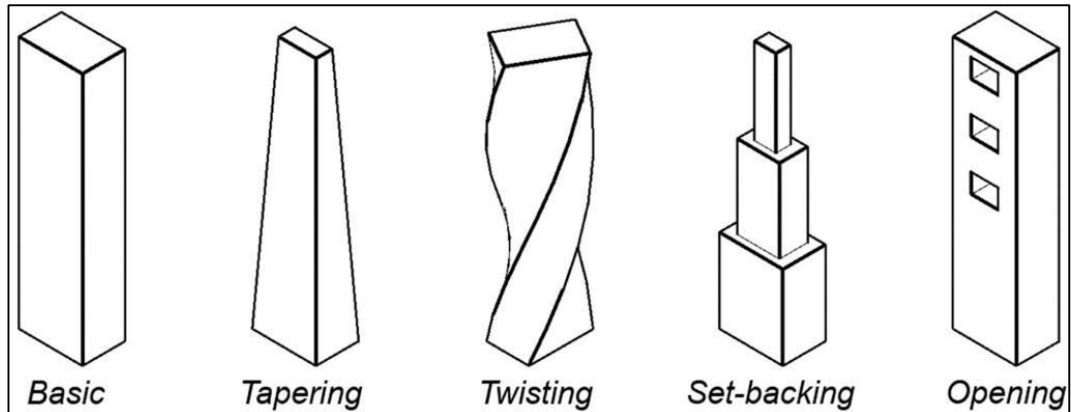


Circuit 3 : Actuator



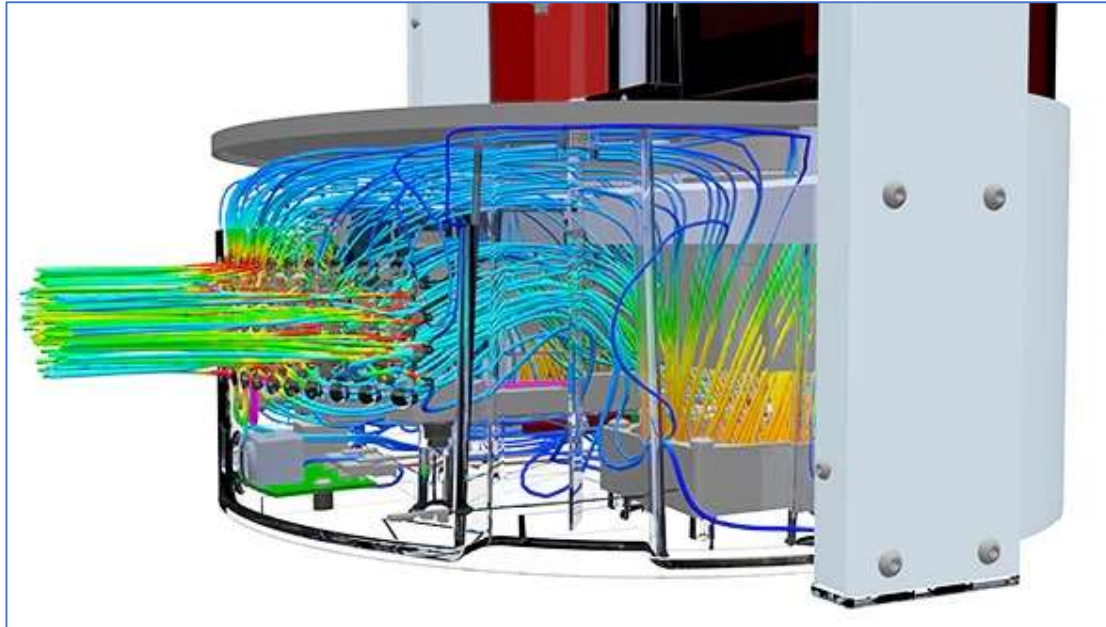
Circuit 4 : Air flow Sensor

## Scope of Development:



Construction of Sky Scrappers





Electronic Circuits

Adaptive aerodynamic bodies offer several significant benefits over conventional static designs. By adapting to changing flow conditions, these systems can optimize their shape to minimize drag, increase lift, and enhance overall performance. This adaptability enables improved efficiency, reduced fuel consumption, increased manoeuvrability, and enhanced safety. The scope of this project report covers a wide range of applications, including but not limited to:

- **Aerospace:** Adaptive wings and control surfaces for aircraft, morphing aircraft structures, and unmanned aerial vehicles (UAVs) with adaptable aerodynamic features.
- **Automotive:** Active aerodynamic systems for cars, such as adjustable spoilers, active grille shutters, and shape-changing body panels.
- **Wind Energy:** Adaptive rotor blades for wind turbines, enabling efficient power generation across a broader range of wind speeds.
- **Sports and Recreation:** Adaptive sports equipment, such as cycling helmets with adjustable aerodynamic profiles or adaptive surfboard fins.

## References:

[https://www.researchgate.net/publication/354252289\\_Reduction\\_of\\_Aerodynamic\\_Drag\\_of\\_Heavy\\_Vehicles\\_using\\_CFD](https://www.researchgate.net/publication/354252289_Reduction_of_Aerodynamic_Drag_of_Heavy_Vehicles_using_CFD) (IJRASET)

<https://www.fleetequipmentmag.com/reducing-truck-trailer-drag-increasing-fuel-efficiency/>

<https://oizom.com/about-technology-environmental-sensors/>

<https://www.fleetequipmentmag.com/reducing-truck-trailer-drag-increasing-fuel-efficiency/>

1. Spalart, P.R., Mclean., J.D.: Drag reduction: enticing turbulence, and then an industry. *Phil. Trans. R. Soc. A* 369, 1556–1569 (2011)
2. Choi, H., Jeon, W.P., Kim, J.: Control of flow over a bluff body. *Annu. Rev. Fluid Mech.* 40, 113–139 (2008)
3. Klumpp, S., Meinke, M., Schröder, W.: Numerical simulation of riblet controlled spatial transition in a zero-pressure-gradient boundary layer. *Flow Turbulence Combust.* 85, 57–71 (2010)
4. Kuya, Y., Takeda, K., Zhang, X., Beeton, S., Pandaleon, T.: Flow separation control on a race car wing with vortex generators in ground effect. *ASME J. Fluids Eng.* 131, 121102 (2009)
5. Huang, R.F., Cheng, J.C., Chen, J.K., Hsu, C.M.: Manipulating flow to reduce drag of a square cylinder by using a self-sustained vibrating rod. *ASME J. Fluids Eng.* 133, 051202 (2011)
6. Ben-Hamou, E., Arad, E., Seifert, A.: Generic transport Aft-body drag reduction using active flow control. *Flow Turbulence Combust.* 78, 365–382 (2007)
7. Krajnovic, S., Östh, J., Basara, B.: LES study of breakdown control of A-pillar vortex. *Int. J. Flow Control* 2, 237–258 (2010)
8. Krajnovic, S., Fernandes, J.: Numerical simulation of the flow around a simplified vehicle model with active flow control. *Int. J. Heat Fluid Flow* 32, 192–200 (2011)
9. Lengani, D., Simoni, D., Ubaldi, M., Zunino, P., Bertini, F.: Application of a synthetic jet to control boundary layer separation under ultra-high-lift turbine pressure distribution. *Flow Turbulence Combust.* (2011). doi:10.1007/s10494-011-9346-z
10. Modi, V.J., Fernando, M.S.U.K., Yokomizo, T.: Moving surface boundary layer control as applied to two-dimensional and three-dimensional bluff bodies. *J. Wind Eng. Ind. Aerodyn.* 38, 83–92 (1991)
11. Modi, V.J., Deshpande, V.S.: Fluid dynamics of a cubic structure as affected by momentum injection and height. *J. Wind Eng. Ind. Aerodyn.* 89, 445–470 (2001)
12. Beaudoin, J.F., Cadot, O., Aider, J.L., Wesfreid, J.E.: Bluff-body drag reduction by extremumseeking control. *J. Fluids Struct.* 22, 973–978 (2006)